University of Tartu

Faculty of Science and Technology

Institute of Chemistry

ANTON RUZANOV

ADSORPTION OF IONS ON Cd(0001) ELECTRODE FROM IONIC LIQUIDS AT DIFFERENT TEMPERATURES

Master's thesis

Supervisors: M. Sc. Vladislav Ivaništšev

Ph.D. Karmen Lust

Tartu 2012

CONTENTS

LIST OF ACRONYMS AND NOTATIONS

RTIL – room-temperature ionic liquid

EIS – electrochemical impedance spectroscopy

$EMImBF_4$ – 1-ethyl-3-methylimidazolium tetrafluoroborate

EDL – electrical double-layer

PZC – potential of zero-charge

DFT – density functional theory

MSA – mean spherical approximation

MD – molecular dynamic

et al. – a Latin term meaning “and others”

ab initio – a Latin term meaning “from first principles”

CV – cyclic voltammetry

AC – alternating current

Z – complex impedance

Z', Z'' – real part and imaginary part of impedance, respectively

δ – phase shift

FMG – classical Frumkin–Melik-Gaikazyan model

MGD – modified Grafov–Damaskin model

R_{el} – electrolyte resistance

C_{dl} – electrical double-layer capacitance

C_{ad} – adsorption capacitance

R_{ad} – adsorption resistance

R_{ct} – charge transfer resistance

Z_w – Warburg diffusion impedance

CPE – constant phase element

INTRODUCTION

Over the last few decades room-temperature ionic liquids (RTILs) have attracted considerable research interest in the fields of surface science and physical chemistry [1]. Wide electrochemical potential and thermal windows, good ionic conductivity, acceptable viscosity, high thermal stability, extremely low vapour pressure and the ability to solubilise many chemical species make RTILs interesting electrolytes for electrochemical applications [2–4]. Compared with commonly used organic compounds, they have low toxicity and are non-flammable. Furthermore, variation of the chemical composition of ions or even just the length of the alkyl groups allows fine tuning of the physicochemical properties of RTILs, such as viscosity, conductivity, catalytic activity, hydrophilicity, melting point etc. Thus, RTILs can be strategically designed for different applications.

Consideration of the structural aspects of RTILs, especially their structure near electrode, is crucial for the rationalization of electrochemical processes in RTILs. Such processes at the RTILs | electrode interface include: diffusion (mass transport), adsorption at the interface (change in surface excess), and charge transfer process across the interface. Experimentally they can be characterized by electrochemical impedance spectroscopy (EIS) in terms of Warburg element, capacitor and resistor, respectively [5–7]. One of these processes dominates and determines the performance of an electrochemical system. The electrochemical processes in RTILs, in their turn, strongly depend on charge, size, polarizability and interactions of RTILs ions at the electrode surface at difference potentials and temperatures. Thus, a deeper understanding of the chemical structure–interface property dependence should benefit the performance enhancement of known electrochemical systems and reveals novel research directions [3,4]. Obviously, it is of practical and theoretical interest to study the potential and temperature dependences of processes at an electrode immersed in different RTIL.

The potential–dependent capacitive processes at different electrodes have been studied for a range of RTILs [8–17]. However, most capacitance measurements were carried out at room temperature and only few systematic analysis of temperature effect were performed [11,12,15,18–20]. In this work EIS was used for characterizing the processes at the interface between 1-ethyl-3-methylimidazolium tetrafluoroborate ($EMImBF_4$) and Cd(0001) electrode at different temperatures.

LITERATURE REVIEW

The development of physics and chemistry during the last century ensured a vast knowledge of adsorption. Although, in general, the humanity is still far from comprehensive understanding of this phenomenon [6]. Adsorption occurs in every single stage of heterogeneous reaction, and its role in electrochemical reactions changes upon any variation in electrode potential and temperature. Examination of the temperature effects is thus of crucial importance for practical purposes, primarily for the development of batteries and fuel cells and also for the development of electrosynthesis methods, corrosion protection, etc. [21]. If in the XX century most electrochemical reactions were carried out in the aqueous solutions, nowadays, a new class of non-aqueous, RTILs serve as a perspective electrolyte for the electrochemistry of future.

Properties of RTIL

RTIL may acceptably be defined as a fluid (at or near room temperature) semi organic salt composed entirely of organic cations and organic or inorganic anions. There is considerable consensus that a qualified RTIL must melt below 100 °C [3]. A tendency to crystallize at low temperatures results from flexibility of anions and dissymmetry of cations [4]. RTILs are basically composed of organic ions that may undergo almost unlimited structural variability [4]. The most common cations are: alkylpyridinium, alkylimidazolium, alkylphosphonium, and alkylammonium, which can combine with anions such as BF_4^-, PF_6^-, NO_3^-, CH_3COO^-, $CF_3SO_3^-$, etc [3].

Physical properties of RTILs strongly depend on their structure. RTILs are more viscous than common molecular solvents and this property is determinate by electrostatic interactions, van der Waals forces and hydrogen bonding. Viscosity of RTILs increases with alkyl chain's length because of stronger van der Waals forces between cations. RTILs have good ionic conductivity, which depends on the number of charge carriers and on their mobility. Precisely as may be anticipated, RTILs with higher viscosity have lower conductivity. RTILs are denser than water and their densities decrease with increase in the length of the alkyl chain in the cation. Also, density is affected by identity of anions. Both chemical structure of anion and cation determines relatively low melting points of RTILs. If anion size increases, the melting point decreases; if cations are large and asymmetrically substituted, the melting point is lowered. Thermal stability of RTILs is mainly limited by the

strength of their heteroatom-carbon and heteroatom-hydrogen bonds. It might be up to 450 °C, but RTILs can tolerate such high temperature only for short time. To sum up, various kinds of anions and cations can be used to design the RTIL that has the desired properties for a given application [4].

Due to their wide electrochemical windows and good ionic conductivities, RTILs have found potential applications in the field of electrodeposition [3,4]. Many metals and alloys that cannot be obtained in aqueous media in most cases can be deposited in RTILs, as hydrogen evolution does not interfere in the case of RTILs. Thus, all metals and alloys can be theoretically electrodeposited in RTILs via designing and selecting reasonable RTILs. Also RTILs show a potential for electrosynthesis as they have a number of distinct electrochemical advantages. For instance, RTILs may act as both solvent and electrolyte, therefore removing the extraneous electrolytes that normally would have to be recovered or recycled after electrolysis. Moreover, RTILs can be designed to dissolve a wide range of substrates and are not restricted to the 'like dissolves like' scenario of molecular solvents. RTILs with many amazing properties are currently used in electrocatalytical fields, not only as reaction media but also as catalysts or electrocatalytic activators [22]. RTILs are also used in other electrochemical applications, such as electrochemical biosensors, electrochemical capacitors, lithium batteries, fuel cells, actuators, solar cells and a number of smart devices yet to be invented [22–27]. Precise control of the interface between the electrode and RTIL solvents allows us to alter the electron transfer and energy storage ability in the devices, and thus improve their performances [3,4,28].

RTILs, such as $EMImBF_4$ (T_{melt} = 15 °C [29]), have been extensively studied since 1990s, mainly because of the rich diversity of their physicochemical properties [1]. A decade later, electrode | RTIL interfaces have attracted considerable attention due to high stability of new types of ionic liquids under applied potential and their decisive role in interfacial processes [2–4]. Non-faradaic potential-driven structure transformations and charge transfer processes at the electrode | RTIL interface are important issues in enhancing the performance of many energy production-storage devices. The interfacial chemical structure of RTILs has also strong influence on faradaic reactions [30]. Therefore, a deeper understating of how RTIL ions change chemical structure of the interface and its properties is vital for more efficient electrodeposition, electrosynthesis and electrocatalysis in RTIL based electrolytes.

Cadmium single crystal electrode

Cadmium is widely used in energy technology for batteries and solar panels production. Cadmium resources are limited; therefore, knowledge of cadmium electrochemistry is certainly very important for its recovery and usage. However, cadmium as a research object is appealing to electrochemists also for an entirely different reason: in a range of potentials, this metal is almost ideally polarisable. Ion adsorption thermodynamics at polycrystalline and monocrystalline electrodes in aqueous solutions has been studied for a long time, but there are still many unresolved issues [30–33]. However, in RTILs cadmium has not been studied at all. Metals with similar characteristics – such as cadmium, mercury, antimony, and bismuth – have high overvoltage and a wide area of ideal polarizability upon hydrogen evolution – the range of potentials where there is no charge transfer through the maximum interfacial surface; which basically means that there are no electrochemical reactions. In addition, there is a metal class with different properties – chemically inactive metals with catalytic properties – Au, Ag, Cu, Pt, Pd and other platinum group metals. There is a third class as well – the one of chemically active metals (Al, Fe, Ti), which have no ideal polarizability in aqueous solutions.

Experimental studies have shown that there is a certain dependence of electrochemical properties on the metal ones. It has been found that the difference between the properties of d-metals and sp-metals results from the different chemical nature of the observed metals, which is logical: owing to low Fermi level, the interaction of solvent molecules with a metal surface is stronger [34–36]. In the case of sd- and sp-metals, the interactions between the metal and the solvent molecules on metal | solution interface are occasionally weaker. At the same time, the properties of sd- and sp-metals prevent electrochemical reactions on surface and allow us to study the adsorption over a wider range of potentials and search for a deeper relation of the adsorption characteristics with the structure of electrical double-layer (EDL) [4,26,28,37].

Electrical double-layer

Undoubtedly RTILs chemistry became one of the present and future trends in modern chemical research. This is evidenced by their appearance in the series “Topics in Current Chemistry” in 2010 [1]. For electrochemistry RTILs present a challenge, as these electrolytes have high charge density, differently from common dilute aqueous electrolytes. This circumstance is important regarding EDL – an interfacial region between metal electrode and

electrolyte where a potential drop occurs. A keen interest in the EDL of RTILs has appeared in ca. 2007, when an influential article titled “Double-layer in ionic liquids: paradigm change?” was published [38]. Main two provisions of this article are still of current interest. Firstly, there is no deep understanding of the structure and properties of the EDL at the metal | RTIL interface. EDL in RTILs cannot be described by the mean-field theory as it is in case of aqueous electrolytes [38]. Secondly, the absence of theoretical models prevents more sensible applications of metal | RTIL interfaces in energy production and conversion devices.

The differential capacitance of the EDL is one of the most important macroscopic properties of all electrochemical systems. Many theories were developed during the XX century that successfully explained the dependence of capacitance on potential of an electrode emerged into a dilute electrolyte [39]. However, the current understanding of capacitance behaviour at metal | RTIL interfaces, that contain high concentration of charge carriers, is limited [39]. Most recently such interfaces attracted much attention due to their high technological potential in various fields of chemistry and physics, and it became evident that their application at electrified interfaces in energy-storage systems, electrocatalysis, deposition and synthesis cannot proceed without a deep understanding of the structure and properties of EDL [30]. Aspects and details related to the electrified interface were addressed by 1) modified Poisson–Boltzmann theory [38,40–43], density functional theory (DFT) [44–47] and mean spherical approximation (MSA) theory [40]; 2) molecular dynamic (MD) simulations [48–56]; 3) experiments at well-defined single crystal electrodes [8–10,12,13,15,19,57,58] and at polycrystalline electrodes [11,14,18,20,59–62]; as well as by few *ab initio* calculations [10,63–66].

On the basis of a Poisson–Boltzmann lattice-gas model, introducing the finite size of the ions, Kornyshev [38], Oldham [43] and Kilic *et al.* [41,42] have developed similar theories describing the diffuse part on the EDL. In simple numerical MD simulations [49,52] was spectacularly proven a general validity of the theories by showing a maximum of the capacitance close to the point of zero charge, which was theoretically predicted. However, both Kornyshev and Oldham admitted that behind beautiful analytical expressions are stated simple assumptions, which are applicable in restricted conditions only and cannot be applied on sole to the whole EDL. It must be stressed, that in most theories there is an empirical parameter describing the closest approach of the adsorbed ions, which describes an inner part of the EDL. In order to describe the differential capacitance behaviour besides the diffuse part

the compact-layer (inner part of EDL) has to be accurately accounted. However, the ratio of the diffuse and inner part capacitances in total differential capacitance for RTILs is still not clear. By the matter of fact, since the times of the Helmholtz, who described the first primitive model, and till nowadays the compact-layer is treated as a planar capacitor neglecting the effects of strong metal–adsorbate interaction as well as its dependence of potential and temperature. Thus, frequently interpretation of experimental results is incomplete due to the limitation of theoretical level involved. For instance Baldelli interpretation stating the EDL is one-layer thick is obviously oversimplified [67]. However, it only means that the role of the compact-layer might be heightened. Controversial statement of Kornyshev, that EDL is more than one-layer thick is based on assumption that the differential capacitance is mostly determined by diffuse layer capacitance. Herewith, this statement is supported by MD simulations [49,52] in which the strength of interactions at the interface is neglected. To sum up, there is a need for new insight on the EDL structure and properties (as capacitance) in order to clarify the role of compact and diffuse layer. Note that probably the division accepted for the EDL at metal | aqueous electrolyte interface is not even valid for metal | RTIL interface.

From chemical point of view, all parameters in any arbitrary equation describing EDL properties are dependent on chemical bonding between species. In MD simulations [51,53,68] accounting “non-electrostatic” interactions has fairly shown, that cation–anion correlations and the significant adsorption of ions on the electrode strongly affect the differential capacitance. It is worthwhile to study these effects at different experimental and computational levels and to incorporate them into the theoretical models of EDL in order to design electrochemical systems with desired properties. An exciting possibility that EDL structural effects may be explained gives confidence that the very diverse trends of capacitance-potential curves observed experimentally may be described and predicted.

Temperature effect studied by EIS

One of the ways to obtain more information about the structure of the EDL at the electrode | RTIL interface is by means of EIS, by studying the temperature dependence of impedance. Nowadays, more and more attention is paid to the differential capacitance dependence on temperature in RTILs at coinage metals and graphite [11,12,15,18–20,61]. In the same time any studies at technological metals, such as cadmium, are rare [3].

Lockett *et al.* [20,61] investigated the EDL properties of glassy carbon electrode and imidazolium-based RTILs: EMImCl, BMImCl, HMImCl[1]. The chloride anion was chosen as a common anion for all liquids because of its simple structure and known behaviour at the solid electrode immersed in aqueous electrolyte or in molten salts. EIS and cyclic voltammetry (CV) were used over wide ranges of potential (ΔE = 2.5–4.0 V) and temperature (from 80 to 140 °C). These were the first determinations of influence of temperature on the differential capacitance of the electrified solid | RTIL interface [20]. Experiment was conducted at different temperatures within the range from 80 to 140 °C. The authors found that the capacitance, measured at constant frequency of 1000 Hz, increases with temperature and showed that the effect is more pronounced on the anodic side of the curve.

Costa *et al.* [18] measured the effect of temperature on the interface between Hg and alkylimidazolium-based RTILs: EMImTf_2N, BMImTf_2N, HMImTf_2N[2]. The experiment was performed at temperature range from 30 to 60 °C. The authors found that the capacitance values, measured at 200 Hz, increase with temperature in the whole potential range for all RTILs studied. Previously similar dependence of the differential capacitance was observed by Silva and Costa *et al.* [11] for the interfaces formed at a solid metal (Pt), a liquid metal (Hg) and a semi-metal (GC) in contact with $BMImPF_6$. These experiments were conducted at different temperatures within the range from 20 to 75 °C.

Most recently Drüschler *et al.* presented their results for the influence of temperature on the differential capacitance of the $Py_{1,4}FAP$[3] | Au(111) interface at temperature ranging from 0 to 90 °C [19]. Differently from other publications, it was claimed that the differential capacitance of the electrode | RTIL interface, obtained by impedance spectra modelling, decreases with temperature increase. The authors showed that careful analysis of broadband impedance spectra results in a very weak temperature dependence of the differential capacitance values. They suggested that capacitance data recorded at a single frequency (as in Ref. [11,18,20,61]) may pretend strong temperature dependence, while the true double layer

---

[1] $EMIm^+$ – 1-ethyl-3-methylimidazolium cation; $BMIm^+$ – 1-butyl-3-methylimidazolium cation; $HMIm^+$ – 1-hexyl-3-methylimidazolium cation; Cl^- – chloride anion.

[2] Tf_2N^- – bis(trifluoromethylsulfonyl)imide anion

[3] $Py_{1,4}FAP$ – 1-butyl-1-methylpyrrolidinium tris(pentafluoroethyl)trifluorophosphate

capacitance may depend on temperature. Drüschler *et al.* clearly showed that the differential capacitance is frequency dependent and that the apparent increase of the differential capacitance with increasing temperature found in single-frequency measurements appears to be an artefact due to the existence of two capacitive processes with temperature-dependent relaxation times [19,57].

The appearance of two or more capacitive processes was described in the works of Kolb *et al.* [12,58] and Siinor *et al.* [9,10]. At $BMImPF_6$ | Au(100) [12] and $EMImBF_4$ | Bi(111) the electric double layer capacitance increases with the rise of temperature. More complex behaviour was found for Au(111) electrode immersed into $EMImBF_4$, $BMImBF_4$ or $HMImBF_4$ [15]. To sum up, rather different temperature dependences may be found for different RTILs in contact with different electrodes. There is no universal and widely accepted explanation to the dependences. Therefore, this research aims to provide new insights to the existing knowledge on the temperature dependence as well as at making new findings with the help of EIS for the Cd(0001) | $EMImBF_4$ interface.

EXPERIMENTAL

Electrodes

A three-electrode setup was used with a high-surface Pt mesh counter electrode, a straight Ag wire coated with AgCl (Ag | AgCl) as a reference electrode, and the Cd single crystal acting as a working electrode. The electrode was prepared from Mateck Cd(0001) single crystal – a cylinder with the diameter of 4 mm. The crystallographic orientation of Cd(0001) was determined by X-ray diffraction method. The final preparation of the electrode was accomplished by electro-chemical polishing in the solution of H_3PO_4 performed before each experiment.

Room Temperature Ionic liquid

$EMImBF_4$ was purchased from Fluka (water content ≤ 200 ppm, high purity over 99.0%). All experiments, including handling of the RTIL, were performed in argon atmosphere. It is important to note that some impurities often observed in commercial RTILs can strongly alter the surface processes leading to misinterpretations [69]. To avoid the influence of impurities we investigated a narrow potential window from –0.5 to –1.0 V, for which cyclic voltammetry do not reveal any noticeable faradaic reactions.

Experiment

EIS was applied to measure the differential capacitance dependence of EDL on the electrode potential (E) and the dependence of complex impedance on the alternating current (AC) frequency (f) at constant potential. The impedance spectra were recorded with Autolab PGSTAT 30 system controlled by the FRA II software. The measuring cell were washed with concentrated sulphuric acid with addition of a small amount of H_2O_2 and heated up to 70 °C degrees. C vs. E curves were measured at fixed values of AC frequency f = 1000, 525, 201, 30 Hz within the potential range from –0.5 to –1.0 V (0.1 V steps). Impedance spectra were measured within the AC frequency range from 0.1 to 10000 Hz at different electrode potentials. Measurements were performed by moving from negative potentials towards positive potentials and from lower temperatures to higher temperatures (t = 30, 40, 50, 60, 70 °C). The dependence of temperature reading within the cell was calibrated with an accuracy of ±1 °C. All impedance measurements were performed inside glove box (Labmaster sp, LMBraun; O_2 and H_2O concentrations < 5 ppm).

MEASUREMENT METHODS

Electrochemical impedance

EIS method is based on the system response to the appeared periodic AC signal with small amplitude. Total impedance Z is a complex value consisting of an imaginary and a real part and can be expressed in polar coordinates

$$Z = |Z|e^{\delta(\omega)}$$

(where $|Z|$ is impedance module and δ – phase angle between the AC and potential applied) and as Cartesian, i.e. the sum of complex variables [5,70]:

$$Z = Z' + Z''$$

where Z' is the real part (real resistance dependent on frequency, $R(\omega)$) and Z'' is the imaginary part called capacitive resistance ($1/(jC\omega)$, where j is imaginary unit and ω is angular frequency ($\omega = 2\pi f$)). So-called Nyquist plot, or Z'', Z'-graph, describes the dependence of the imaginary part on the real part. The dependences of complex impedance and phase shift (δ) on frequency are called Bode plots. The graphs not only provide a quick qualitative overview of experimental data, but can also be used for the quantitative analysis by means of different models.

Complex impedance module divided into the real and imaginary parts as follows [70]:

$$|Z|^2 = (\mathrm{Re}\ Z)^2 + (\mathrm{Im}\ Z)^2 = (Z')^2 + (Z'')^2.$$

where

$$\mathrm{Re}(Z) = |Z|\cos\delta \quad \text{and} \quad \mathrm{Im}(Z) = |Z|\sin\delta.$$

Impedance modelling

Modelling of impedance spectra allows obtaining information on the regularities of the adsorption, diffusion, and charge transfer processes on the electrode. Using EIS method of studying anion adsorption kinetics on the Cd(0001) and Bi(111) [33] electrodes in aqueous solutions and on the Bi | $BMPyBF_4$[4] interface [10], it has been found that in order to be able to

[4] $BMPyBF_4$ – 1-butyl-4-methylpyridinium tetrafluoroborate

model experimental dependencies as well as to explain the essence of physical processes, a classical Frumkin–Melik-Gaikazyan (FMG) model (**Circuit a**) can be used:

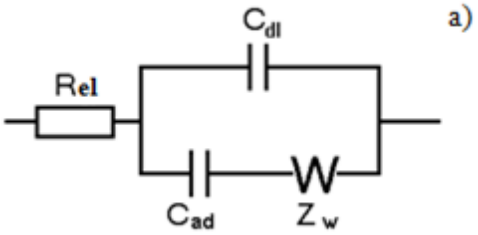

where the adsorption capacitance (C_{ad}) and Warburg (diffusion) impedance (Z_W) are connected in parallel with EDL capacitance (C_{dl}). Z_W characterises a diffusion stage of the process or slowness of the mass transfer step. This circuit can describe some processes in RTILs as well. The circuit also includes resistance (R_{el}), which can be found by extrapolation – of the Z'', Z' dependencies to high frequencies.

The FMG model impedance [70] is expressed as follows:

$$Z_{\mathrm{FMG}}(\mathrm{j}\omega) = R_{\mathrm{el}} + \frac{1}{\mathrm{j}\omega C_{\mathrm{dl}} + \dfrac{1}{Z_{\mathrm{W}} + \dfrac{1}{\mathrm{j}\omega C_{\mathrm{ad}}}}}$$

Generally, finite-length Warburg impedance [70] is expressed as follows:

$$Z_{\mathrm{W}} = \frac{R_{\mathrm{D}}}{(\mathrm{j}\omega T)^{\alpha_{\mathrm{W}}}} \tanh(\mathrm{j}\omega T)^{\alpha_{\mathrm{W}}}$$

where R_D is diffusion resistance; T is so-called mass transfer frequency coefficient that characterises the thickness of the diffusion layer, and α_w is diffusion constant – the exponent that characterises diffusion equilibrium.

A modified Grafov-Damaskin (MGD) model (**Circuit b**) is used for ion adsorption modelling, which takes into account the processes occurring at the electrode (R_{ct} – partial charge transfer resistance). If $R_{ct} \rightarrow \infty$, we get the classical FMG model.

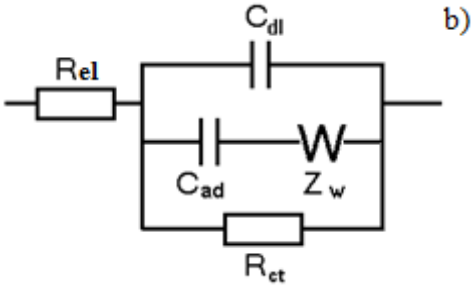

The applicability of FMG and MGD depends on the electrode potential applied. FMG does not give quite good fitting if the slow parallel faradic reactions occur on electrode. However, MGD gives a good fitting within the whole potential range studied and therefore the parameters obtained using this model were analysed in details.

The MGD impedance is expressed as follows:

$$Z(j\omega) = \mathrm{R_{el}} + \frac{1}{j\omega C_{\mathrm{dl}} + \dfrac{1}{\dfrac{1}{j\omega C_{\mathrm{ad}}} + Z_{\mathrm{W}}} + \dfrac{1}{\mathrm{R_{ct}}}}$$

In several studies [13,58], the following scheme has been used for modelling, where *R* (in this case, *R* is marked with index *ad*) is serially to Warburg diffusion impedance (Z_{w}) and adsorption capacitance (C_{ad}) (**Circuit c**).

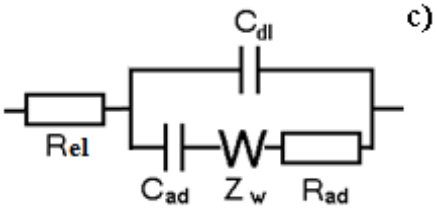

Some researchers have concluded that the interfacial impedance can be modelled by this equivalent circuit [58], giving the R_{ad} parameter the meaning of a resistance of the interfacial layer towards adsorption process, i.e. reorganization of EDL. It is worth to notice, that the same meaning may be attributed to the R_{ct} in the circuits above. Whether it is a true Faradic process or non-Faradic adsorption, the charge transfer over the dense interfacial layer is complicated. The temperature dependence of low frequency resistance (R_{ad} or R_{ct}) is related to the structural peculiarities of the EDL in RTILs.

In many studies [13,20,62,71,72] for a good fitting of experimental data researchers used schemes, which contain constant phase element (CPE). The CPE represents the

frequency-dispersed version of the double-layer capacitance (C_{dl}) and originates from the spatial inhomogeneity of the electrode interface. Uneven packing of the large, asymmetric cations of the RTIL in double layer contributes to these interfacial inhomogeneities.

According to the IUPAC recommendations [79] the admittance ($Y = Z^{-1}$) of CPE [70] is given by

$$Y_{\mathrm{CPE}} = Y_0 (i\omega)^n$$

where n is a number from –1 to +1; for solid electrode | solution interface $0.5 < n < 1$, Y_0 is a constant with units $\Omega^{-1}\mathrm{m}^{-2}\mathrm{s}^n$, which becomes equal to the double-layer differential capacitance ($Y_0 = C_{dl}$) at $n = 1$. Both n and Y_0 are dependent on the electrode potential, temperature, ionic concentrations and electrode roughness [20]. Only when $n = 1$ does the CPE behave as a pure capacitor and when $n \rightarrow 0.5$ it acts as a Warburg element indicating diffusion limited kinetics [5].

EXPERIMENT RESULTS

Cyclic voltammetry

CV (20 mV/s) was used to verify the double layer region free form electrode reactions, cleanness of the ionic liquid and reproducibility of the system. It was also performed at the end of each impedance measurement to control the stability of the system. The area of the low current is larger from the side of less negative potentials (in the absence of H_2 evaluation) compared to the aqueous solutions. **Figure 1** shows three cyclic voltammograms of Cd(0001) electrode in contact with $EMImBF_4$. Significant cathodic and anodic faradic currents rice beyond –1.2 V and –0.4 V (CV1 and CV2), respectively. At anodic potentials dissolution of Cd electrode takes place, which is visually observable. At cathodic potentials a reaction of water impurity occurs. We limited our EIS measurements to a narrow region from –1.0 V to –0.5 V (CV3) to avoid these faradaic processes.

Nyquist (Z'', Z') and Bode (δ, f) plots

The electrochemical impedance analysis provides information on which of the stages is most likely to be the limiting: adsorption, i.e. double-layer reorganization; diffusion of the species towards and outwards the electrode surface; or charge transfer process.

Figure 2a shows Z'', Z' dependencies for five experiments at fixed temperature and potential (t = 30 °C, E = –0.8 V). The real part of impedance (Z') corresponds to the resistance. The impedance spectra is significantly influenced by the course of unwanted processes, which we tried to model by charge transfer resistance R_{ct}. The value of R_{ct} depends on preparation procedure of experiment and most probably is sensitive to the concentration of water impurity. In spite of significant deflection of all experimental results from each other at low frequencies (f < 15 Hz), at high frequencies it is clearly seen that the curves of all experiments coincide (inset in **Figure 2a**). Consequently the fast capacitive process of EDL formation (C_{dl}) reproduces with a good accuracy from experiment to experiment. However, the slow capacitive process associated with the reorganization of the EDL is significantly influenced by changeful slow process modelled by R_{ct}. **Figure 2b** shows Y''/f, Y'/f dependencies at different temperatures at fixed potential (E = –0.8 V). The real part of admittance (Y'/f) corresponds to the capacitance values. It is possible to observe the deviation of the measured admittance from the ideal semicircle (dotted lines), which indicates the significant effect of mass transfer process [75]. The latter process was modelled by Warburg

impedance.

The proportion of stages determining the speed of the process can be assessed with the phase angle δ based on the dependence on the AC frequency (**Figures 3** and **4**). At high AC frequencies the fast EDL charging occurs. Herewith, this process is hindered by the electrolyte resistance. At low AC frequencies, on the other hand, the absorption is hindered by mass transfer (diffusion) and charge transfer processes. **Figures 3** and **4** show that at very low AC frequencies the charge transfer is dominating as $\delta \rightarrow 0°$. In the all potential range, in low-frequency areas, δ vs. *f* curves demonstrate the dependence on temperature. The higher the temperature, the more is the speed determined by charge transfer. Such dispersion is clearly seen in the case of more negative potentials (**Figures 4a** and **4b**). At potentials $E = –0.5$ V and $E = –0.6$ V the dependence on temperature is within the experimental error. At 10–100 Hz all systems have nearly adsorptive behaviour ($\delta \leq –80°$) (**Figure 4**), and the lower the temperature, the higher absolute value of δ, which is best seen at more negative potentials (**Figures 4a** and **4b**).

EIS MODELLING RESULTS

Modelling circuits of experimental data

Experimental impedance data were mainly modelled using the equivalent circuits illustrated in **Figure 5**, where R_{el} is electrolyte resistance, C_{dl} and C_{ad} are double-layer and adsorption capacitances, respectively; Z_W is Warburg-like diffusion impedance, R_{ad} is adsorption resistance and R_{ct} is partial charge transfer resistance; CPE is constant phase element.

There are two parameters, which give indication of how well the modelling circuit reproduces the experimental data set: (1) an estimate for relative error (in %) of a given element value; (2) the chi-square function χ^2 and the weighted sum of the squares (Δ^2).

The difference between equivalent circuits is presented in the table:

	t / °C	E / V	Circuit a	Circuit b	Circuit c	Circuit d
$\chi^2 \times 10^3$	30	–1.0	12.3	4.5	12.4	2.2
Δ^2	30	–1.0	2.22	0.80	2.20	0.39
$\chi^2 \times 10^3$	30	–0.5	27.2	7.8	27.3	2.9
Δ^2	30	–0.5	4.76	1.35	4.76	0.51
$\chi^2 \times 10^3$	70	–1.0	19.8	2.55	6.3	12.3
Δ^2	70	–1.0	3.69	0.44	1.08	2.22
$\chi^2 \times 10^3$	70	–0.5	19.9	9.3	20.0	13.9
Δ^2	70	–0.5	3.48	1.61	3.48	2.69

At negative potentials the MGD model (**Figure 5b**) proved to be the most appropriate, where in addition to the slow adsorption phase (which describes adsorptive capacitance C_{ad}), some slow mass transfer in the adsorbed layer (adescribed by Z_W) is taken into account.

R_{ct} characterises a charge transfer taking place in parallel with the slow adsorption stage. R_{el} describes bulk resistance of the RTIL. Circuit (**b**) was used for the modelling of all experimental data, because it proved to give lowest values of χ^2 and Δ^2 at all potentials and temperatures.

Differential, electrical double-layer and absorptive capacitances

Differential capacitance (C_d) is a parameter that characterizes the EDL capacitive properties:

$$C_d = \frac{\partial q}{\partial E};$$

where q is the charge density at the electrode and E is the electrode potential.

EIS modelling allows dividing the differential capacitance into components. At the frequency $f \rightarrow 0$, differential capacitance is a sum of C_{dl} and C_{ad}. C_{dl} is high-frequency, electrical double-layer capacitance, which occurs at constant surface excess (Γ). The absorption capacitance (C_{ad}) is expressed as as:

$$C_{ad} = (C_0 - C_{dl}) = \left(\frac{\partial q}{\partial \Gamma}\right)_E \left(\frac{\partial \Gamma}{\partial E}\right)_\mu$$

where thermodynamic low-frequency capacitance being expressed as follows:

$$C_0 = \left(\frac{\partial q}{\partial E}\right)_{\Gamma,\mu} + \left(\frac{\partial q}{\partial \Gamma}\right)_E \left(\frac{\partial \Gamma}{\partial E}\right)_\mu$$

C_{ad} appears due to the fact that the surface excess of ions depends on the electrode potential.

The dependence of the modelled capacitance on frequency in terms of C_{dl} and C_{ad} is expressed as follows:

$$C(\omega) = C_{dl} + \frac{1}{j\omega R_{ct}} + \frac{C_{ad}}{1 + C_{ad}\sigma_{ad}\sqrt{j\omega}}$$

Commonly discussed, the differential capacitance (C_d) (**Figure 6a**) is measurable directly at constant frequency. Its dependence on the potential of the Cd(0001) electrode in RTIL and can be related to the structure of the ionic liquid near the surface. The adsorption capacitance (C_{ad}) and the electrical double-layer capacitance (C_{dl}) values are obtained by means of modelling the impedance spectra (**Figure 6b**). **Figure 6c** shows that the adsorption

capacitance at Cd(0001) electrode has a maximum at E = –0.8 V where most probably the PZC area is located. In contrast, C_d has minima at this potential, which is most clearly seen at higher temperatures. The explanation to this observation is given in the discussion section. The dependence of C_{dl} and C_{ad} on temperature is good to follow in **Figure 7**: capacitances show increase with increasing temperature indicating that the EDL structure depends on temperature as well. It should be noted, that the impedance representation as a series of *R*-*C* reveals, that an accurate division of C_{dl} and C_{ad} capacitances is rather complicated (**Figure 8**). The capacitance value depends strongly on frequency and it is difficult to divide it to some parts, as at low frequencies it is hindered by charge transfer resistance (R_{ct}) and at high frequencies by electrolyte resistance (R_{el}).

Partial charge transfer resistance and diffusion resistance

In Figure 9a the dependences of charge transfer resistance (R_{ct}) on temperature and electrode potential are shown. R_{ct} has maximal values at E = –0.5 V and E = –0.6 V decreasing towards more negative potentials. That is why at Bode plots there is practically no temperature dependence at these potentials. R_{ct} decreases with increasing temperature according to Arrhenius law. Estimated Van't Hoff's coefficient does not depend on the potential and varies within the range from 1.3 to 1.4.

Figure 9b shows that the dependence of the diffusion resistance (R_D) (calculated from Warburg impedance) on temperature. Although the diffusion coefficient increases by an order of magnitude within the temperature range [73,74], there is no clear temperature dependence. This indicates that the diffusion layers structure remains unchanged, while the interfacial structure modelled by R_{ct} most probably experiences temperature-driven reconstruction. R_D dependence on electrode potential also provides a strong clue for the position of the PZC, at E = −0.8 V, at which the electric field is minimal and thus charged species are less attracted by the electrode surface.

DISCUSSION

The effect of increasing temperature is expressed in the increase of the differential capacitance (C_d) and the EDL capacitance (C_{dl}) in the whole potential range for $EMImBF_4$ | Cd(0001) interface (**Figures 6a** and **6b**). Similar temperature dependence of C_d on temperature for RTIL | electrode interface has also been observed by Silva *et al.* [11], Lockett *et al.* and Costa *et al.* [18]. Silva *et al.* suggested that an increase in the concentration of "free" ions as a consequence of the breakdown of ionic pairs plays a significant role in the temperature induced changes of the C_d. Similarly, Lockett *et al.* proposed that the growth and change in the *C* vs. *E* curves with temperature is likely initiated by decreased ion association in the double-layer with increasing temperature. Costa *et al.* suggested a possible multilayer structure for the RTIL | electrode interface that may be formed by interpenetrating layers of cations and anions facilitated by various types of possible interactions, which may react towards an increase in temperature to increase the number density of "free" ions or allowing a closer approach of the layers towards the surface.

Exploration of such a temperature dependence of C_d (**Figure 6a**) can be divided into the following complementary parts, based on the following keypoints: 1) modern understanding of EDL structure at electrode | RTIL interface, 2) recent theoretical descriptions of EDL, 3) novel models in interpretation of experimental results.

Modern understanding of EDL structure at electrode | RTIL interface

Starting from year 2007 a number of scanning tunnel microscopy (STM) studies have revealed ordered structures at charged electrodes [12,75–78]. Some years latter atomic force microscopy (AFM) data suggested that the RTIL structure represents a well-ordered region near at electrode surface (**Figure 10**) [17,78–80]. The first bilayer adjacent to the solid surface is considerably denser than the others. It consists of cations and anions forming two layers: one of counter-ions with charge opposite by sign to electrodes charge and another of co-ions. Counter-ions charge density over-screens the co-ions charge density, thus co-ions repulsion from the charged surface is less pronounced, than might be expected. Second layer and consequent bilayers have similar divisions in counter and co-ions layers, however, with less order. Also the magnitude of the charge densities of counter-ions and co-ions (relative to the charge densities of cations and anions in the bulk) decrease at a distant from the electrode. Specific structure of the RTIL provides excellent electrostatic screening at distance of 1–2 nm

[81], therefore less than in common aqueous electrolyte solutions. The depth of the interfacial structure propagation into the bulk liquid depends on the chemical structure of the RTIL, potential, temperature and impurities [78]. The relative magnitude of charge density in RTIL surface decreases with temperature as it was shown in recent MD simulations [50,54,55]. MD studies confirm that the electrode | RTIL interface structure represents a well-ordered region, in which cations and anions form alternating layers. Dou *et al.* [55] found in their MD simulation of graphite | $BMImPF_6$ interface, that the peaks related to the well-ordered surface structure become weaker and the third and fourth layers even disappear with the increase of temperature from 400 to 800 K. The same interface was studied by Kislenko *et al.* [50] in somehow lower temperature range from 300 K to 400 K. In general MD, AFM and EIS studies supplement each other revealing that the dynamics of ions is very slow with glass-like structured behaviour of the RTIL near the surface (innermost, i.e. first bilayer) at low temperatures and high voltages and becomes faster or even comparable to the dynamics of the bulk with the rise of temperature and near PZC.

Theories of EDL at electrode | RTIL interface

Division of the EDL into Helmholtz and diffuse layer in RTILs is unjustified due to layered interface structure. The innermost layer obviously gives highest impact to the capacitance of the EDL:

$$C = \frac{\varepsilon\varepsilon_0}{d}$$

where, at zeroth approximation, d is the distance of closest approach of ions in contact with the surface, i.e. the distance from the electrode surface to the centre of counter-ions layer; ε is relative dielectric constant; ε_0 is permittivity of vacuum. Thus, in this form the Helmholtz layer capacitance figurate in several modern theories [38,82] and is constantly recalled to explain the experimental results for RTIL | electrode interface [20,59,60,67]. Assume, that at a given potential with the rise of temperature the distance changes only slightly, which is anticipated from MD studies [50,55]. Then the dielectric constant should grow until it reaches the value of the bulk dielectric constant, as with thermal distortion ions gain more degrees of freedom. The bulk dielectric constant is known to decrease with temperature increase according to Kirkwood's formula [83]. Thus, it can be expected qualitatively, that the capacitance increases with increase of temperature until some critical temperature, at which

the layered interfacial structure would be broken down.

According to MSA theory [40], differential capacitance can be expressed as:

$$C = \frac{\varepsilon\varepsilon_0}{2\pi}\Gamma$$

where

$$\Gamma = \frac{d\sqrt{1+\kappa}-2}{2d} \sim \kappa$$

is a renormalized screening constant. Here κ is the Debye screening parameter and d is the diameter of ions. Simple MSA predicts decrease of the capacitance as $\kappa \sim \sqrt{(1/T)}$ (Taylor series expansion) [84]. But when association of ions is taken into account via mass-action law (MAL), at relatively low temperatures, the increase of capacitance takes place as briefly explained further. In combined MSA-MAL theory the RTIL is considered to be a mixture of free ions and complex ionic aggregates, among which only an ionic pair is taken into account as most simple one. The charge density of ions is divided into the density of free and bound parts, respectively: $\rho=\rho_0+\rho_{pair}$. Defining $\alpha=\rho/\rho_0$, the MAL is expressed as:

$$\frac{1-\alpha}{\alpha^2} = \frac{1}{2}\rho K_A$$

where K_A is the equilibrium constant for ion-pair formation process. This will lead to the corrected renormalized screening constant, defined as:

$$\Gamma = \frac{d\sqrt{1+\kappa\sqrt{\alpha}}-2}{2d} \sim \kappa\sqrt{\alpha}$$

At high temperatures, $\alpha \rightarrow 1$ and thus a classical behaviour of capacitance on temperature is expected [84]. At lower temperatures, $\alpha \rightarrow 0$ which implies a change of the temperature dependence. Qualitatively this theory predicts behaviour observed in this work. However the main assumption of ion association has to be justified. To constitute the need for accounting the ion-pair formation, firstly, we have to keep in mind that ρ_0 is related to the surface excess of ions. Secondly, from a structural view, the directionality of ion-pair by the H-bond formation results of fast and slow dynamics in RTIL bulk [85]. Due to correlation of ions, at least in imidazolium based RTILs, at a given moment most ions can be grouped in pairs, although, the hydrogen bonds are too weak to hold these pairs for a long time [86]. The

correlation is distorted by high temperature giving more degrees of freedom to the interfacial structure and releasing free ions.

It should be noted that two different interpretations give results in similar qualitative description, while the first considers mainly relative permittivity, the second – only effective distance in terms of renormalized screening constant.

Generalized approach was recently proposed by Feng *et al*. [87] in a framework of ‘‘counter-charge layer in generalized solvents’’ (CGS) model. Within the CGS approach, the effective quantity ε/d is expressed as follows:

$$\frac{\varepsilon}{d} = \frac{1}{d_0 + \sum_{i=1}^{N} (-1)^i \gamma_i \Delta_i}$$

where d_0 is the distance of closest approach of ions in contact with the surface, i.e. the distance from the electrode surface to the centre of counter-ions layer; ε is dielectric constant; $\gamma_i\Delta_i$ are calculated numerically based on data obtained from MD simulation and have the meaning of charge over-screening multiplied by the average distance between the counter-ion and co-ion of the *i*-th layer. As $\gamma_i\Delta_i$ decreases with *i*, the dielectric screening inside EDL is mainly controlled by the first few EDL layers. If there would be only one layer, the capacitance would be equal to $\varepsilon\varepsilon_0/d_0$. Two layers would increase effective dielectric constant and thus the capacitance to the value calculated as: $\varepsilon\varepsilon_0/(d_0 - \gamma_1\Delta_1)$. However, the third layer would decrease its value, respectively: $\varepsilon\varepsilon_0/(d_0 - \gamma_1\Delta_1 + \gamma_2\Delta_2)$. In a reverse order, under thermal distortion, the disappearance of the third layer would result in capacitance incensement until only two layers would remain, and then disappearance of the second layer would lead to capacitance decrease.

Interpretation of experimental results

Three explanations presented are based on: 1) phenomenological theory, 2) MSA-MAL approximation and 3) MD simulation based approach, respectively. They are in agreement with a vast number of experimental, theoretical and computational studies, as well as with EIS data collected during this study. Therefore, it cannot be concluded, that observed capacitance increase with the rise of temperature is related to the changes in the interfacial structure of RTIL | electrode interface caused by the rise of temperature. This phenomenon results from distortion of electrostatic interactions between the ions by thermal excitation and

may be described as subsequent dissolution of EDL layered structure.

Another evidence of complex and most probable multilayered structure comes from R_{el} and R_{ct} analysis. As seen in **Figure 11**, R_{el} and R_{ct} depend strongly on temperature indicating that these are kinetics-related elements. The slope of the log(R_{el}) and log(R_{ct}) vs. 1000/T curve is related to the activation energies E_{el} and E_{ct}. Calculated E_{el} and E_{ct} are equal to 8 kJ/mol and 12 kJ/mol, respectively. Despite the fact, that it does not know the exact nature of charge transfer process, R_{ct} dependence on temperature characterizes the structure of the RTIL layers close to the electrode surface. It is not surprising, that the R_{ct} has higher activation barrier than R_{el}. This means, that the EDL structure is more ordered, than the bulk. Estimated activation energy is in agreement with the value calculated on the basis of conductivity measurements data [73,74]. The ration E_{ct}/E_{el} = 1.5 equals to the same value estimated in experiment of Kolb *et al.* [12]. Surprisingly, the absolute value for E_{ct} is also equal to that found in recent MD simulations [81]. This indicates that all processes happening at the interface are slower, than ions motion in the bulk, due to more ordered structure of the EDL.

It is interesting the compare the results gained at Cd(0001) to those measured at other metals. $EMImBF_4$ has been studied at Au(111) and Bi(111) electrodes. It may be concluded that the capacitance value on three metals is almost equal. However it is not obvious in case of gold, as Alam *et al*. have measured the capacitance at constant frequency value (f = 25 Hz). Such approach has been recently criticized by Drüschler and Kolb, as it does not allow separating capacitances appearing due different processes.

Kolb *et al.* have analyzed the impedance data using **Circuit c** (**Figure 5c**), while Düschler analyzed the impedance data using Cole-Cole method. Both approaches were tested, showing that in principle both give similar results. Even thought, the interpretation might be different. That there are at least two processes at the interface observable by EIS. Kolb attributes the faster process happening faster than in μs to fast redistribution of ions in EDL, and slower processes to the movement of ions in and out of the EDL. Drüschler assumes that the fast processes govern the movement of ions near the surface, but outside the innermost layer of RTIL. He also points to the possibility of an influence of the gold surface reconstructions. And it should be reminded about the impurities, which may and do give rise to slow faradaic processes in certain conditions.

SUMMARY

Cyclic voltammetry and electrochemical impedance spectroscopy (EIS) methods were used for characterizing the processes at the interface between ionic liquid 1-ethyl-3-methylimidazolium tetrafluoroborate and a Cd(0001) electrode at different electrode potentials and temperatures. Such measurements are important for understanding of the structure of the electrode | room-temperature ionic liquid (RTIL) interface.

Analysis of the dependence of the capacitive resistance on the active resistance component (so-called Nyquist plot) shows reproducibility between the experiments. At low frequencies a significant deflection of all experiment results from each other observed, but at high frequencies it is clearly seen that the curves of all experiments coincide quite good. Dependence of the phase angle on the alternating current (AC) frequency shows that at high AC frequencies the fast electric double-layer charging occurs; at low AC frequencies, however, the absorption is hindered by mass transfer (diffusion) and charge transfer processes. In the all potential range, in low-frequency areas, δ vs. f curves demonstrate the dependence on temperature. The higher the temperature, the higher is the speed determined by charge transfer. At 10–100 Hz all systems have nearly adsorptive behaviour and the lower the temperature, the higher the absolute value of δ.

The impedance data was analysed by fitting the EIS spectra with the help of modified Grafov-Damaskin model. The results indicate a dependence of the Cd(0001) | RTIL interface parameters on the temperature. It was found that double-layer capacitance (C_{dl}) and adsorption capacitance (C_{ad}) increase with increasing temperature, indicating that the double-layer structure depends on temperature as well. The potential of zero charge (PZC) is located near E = –0.8 V where C_{ad}, C_{dl} and R_D have a maximum. C_{ad} and C_{dl} are hindered by partial charge transfer resistance (R_{ct}) and at high frequencies by electrolyte resistance (R_{el}), respectively. Both R_{el} and R_{ct} depend strongly on temperature indicating that these are kinetics-related elements. Calculated activation energies are equal to E_{el} = 8 kJ/mol and E_{ct} = 12 kJ/mol. Small difference in activation energies reveals, that the dependence of R_{ct} on temperature characterizes the structure of the RTIL layers close to the electrode surface, which is denser, than the structure in the bulk.

The RTIL structure represents a well-ordered region near an electrode surface. This structure depends on the chemical structure of the RTIL, potential, temperature and

impurities. Many studies reveal that the dynamics of ions is very slow with glass-like structured behaviour of the RTIL near the surface at low temperatures and high voltages and becomes faster with the rise of temperature and near PZC. That how the structure of metal | RTIL interface depends on temperature may describe several modern theories. One of them is combined MSA-MAL[5] theory. According to it at high temperatures capacitance decrease, but at lower temperatures it increases with the rise of temperature. Qualitatively this theory predicts behaviour observed in this work. However, to justify it more clearly the interface between metal electrode and RTILs should be investigated in more detail by *in situ* methods.

[5] MSA – mean spherical approximation; MAL – mass-action law.

REFERENCES

[1] B. Kirchner, Ionic Liquids, Springer Verlag, 2010.

[2] M. Galiński, A. Lewandowski, I. Stępniak, Ionic liquids as electrolytes, Electrochim. Acta. 51 (2006) 5567–5580.

[3] H. Liu, Y. Liu, J. Li, Ionic liquids in surface electrochemistry, Phys. Chem. Chem. Phys. 12 (2010) 1685.

[4] M. Armand, F. Endres, D.R. MacFarlane, H. Ohno, B. Scrosati, Ionic-liquid materials for the electrochemical challenges of the future, Nat. Mater. 8 (2009) 621–629.

[5] E. Barsoukov, J.R. Macdonald, Impedance spectroscopy: theory, experiment, and applications, LibreDigital, 2005.

[6] Б. Дамаскин, О. Петрий, Г. Цирлина, Электрохимия, Химия М., 2001.

[7] F. Scholz, Electroanalytical Methods: Guide to Experiments and Applications, Springer, 2002.

[8] L. Siinor, K. Lust, E. Lust, Electrical Double Layer Structure at Bi (111) | 1-ethyl-3-methyl-imidazolium Tetrafluoroborate Interface, ECS. Thans. 16 (2009) 559.

[9] L. Siinor, K. Lust, E. Lust, Influence of anion composition and size on the double layer capacitance for Bi(111) | room temperature ionic liquid interface, Electr. Commun. 12 (2010) 1058–1061.

[10] L. Siinor, C. Siimenson, V. Ivaništšev, K. Lust, E. Lust, Influence of cation chemical composition and structure on the double layer capacitance for Bi(111) | room temperature ionic liquid interface, J. Electroanal. Chem. 668 (2012) 30–36.

[11] F. Silva, C. Gomes, M. Figueiredo, R. Costa, A. Martins, C.M. Pereira, The electrical double layer at the [BMIM][PF6] ionic liquid/electrode interface: Effect of temperature on the differential capacitance, J. Electroanal. Chem. 622 (2008) 153–160.

[12] M. Gnahm, C. Müller, R. Répánszki, T. Pajkossy, D.M. Kolb, The interface between Au(100) and 1-butyl-3-methyl-imidazolium-hexafluorophosphate, Phys. Chem. Chem. Phys. (2011).

[13] M. Gnahm, T. Pajkossy, D.M. Kolb, The interface between Au(111) and an ionic liquid, Electrochim. Acta. 55 (2010) 6212–6217.

[14] M.T. Alam, M.M. Islam, T. Okajima, T. Ohsaka, Capacitance Measurements in a Series of Room-Temperature Ionic Liquids at Glassy Carbon and Gold Electrode Interfaces, J. Phys. Chem. C. 112 (2008) 16600–16608.

[15] M.T. Alam, J. Masud, M.M. Islam, T. Okajima, T. Ohsaka, Differential Capacitance at Au(111) in 1-Alkyl-3-methylimidazolium Tetrafluoroborate Based Room-Temperature Ionic Liquids, J. Phys. Chem. C. 115 (2011) 19797–19804.

[16] M.T. Alam, M. Mominul Islam, T. Okajima, T. Ohsaka, Measurements of differential capacitance in room temperature ionic liquid at mercury, glassy carbon and gold electrode interfaces, Electr. Commun. 9 (2007) 2370–2374.

[17] R. Atkin, N. Borisenko, M. Drüschler, S.Z. El Abedin, F. Endres, R. Hayes, et al., An in situ STM/AFM and impedance spectroscopy study of the extremely pure 1-butyl-1-methylpyrrolidinium tris(pentafluoroethyl)trifluorophosphate/Au(111) interface: potential dependent solvation layers and the herringbone reconstruction, Phys. Chem. Chem. Phys. 13 (2011) 6849.

[18] R. Costa, C.M. Pereira, F. Silva, Double layer in room temperature ionic liquids: influence of temperature and ionic size on the differential capacitance and electrocapillary curves, Phys. Chem. Chem. Phys. (2010).

[19] M. Drüschler, N. Borisenko, J. Wallauer, C. Winter, B. Huber, F. Endres, et al., New insights into the interface between a single-crystalline metal electrode and an extremely pure ionic liquid: slow interfacial processes and the influence of temperature on interfacial dynamics, Phys. Chem. Chem. Phys. 14 (2012) 5090–5099.

[20] V. Lockett, R. Sedev, J. Ralston, M. Horne, T. Rodopoulos, Differential Capacitance of the Electrical Double Layer in Imidazolium-Based Ionic Liquids: Influence of Potential, Cation Size, and Temperature, J. Phys. Chem. C. 112 (2008) 7486–7495.

[21] X.-Z. Yuan, C. Song, H. Wang, J. Zhang, Electrochemical Impedance Spectroscopy in PEM Fuel Cells: Fundamentals and Applications, Springer, 2009.

[22] S. Passerini, W.A. Henderson, Secondary Batteries – Lithium Rechargeable systems | Electrolytes: Ionic Liquids, in: Encyclopedia of Electrochemical Power Sources, Elsevier, Amsterdam, 2009: pp. 85–91.

[23] T. Torimoto, T. Tsuda, K. Okazaki, S. Kuwabata, New Frontiers in Materials Science

Opened by Ionic Liquids, Adv. Mat. 22 (2010) 1196–1221.

[24] J. Schaefer, Y. Lu, S. Moganty, P. Agarwal, N. Jayaprakash, L. Archer, Electrolytes for high-energy lithium batteries, Appl. Nanosci. 2 (2012) 91–109.

[25] B. Li, L. Wang, B. Kang, P. Wang, Y. Qiu, Review of recent progress in solid-state dye-sensitized solar cells, Sol. Energ. Mat. Sol. C. 90 (2006) 549–573.

[26] Y. Su, Y. Fu, Y. Wei, J. Yan, B. Mao, The Electrode/Ionic Liquid Interface: Electric Double Layer and Metal Electrodeposition, Chem. Phys. Chem. 11 (2010) 2764–2778.

[27] F. Endres, O. Höfft, N. Borisenko, L.H. Gasparotto, A. Prowald, R. Al-Salman, et al., Do solvation layers of ionic liquids influence electrochemical reactions?, Phys. Chem. Chem. Phys. 12 (2010) 1724.

[28] H. Weingärtner, Understanding Ionic Liquids at the Molecular Level: Facts, Problems, and Controversies, Angew. Chem. Int. Edit. 47 (2008) 654–670.

[29] S. Zhang, X. Lu, Q. Zhou, X. Li, X. Zhang, S. Li, Ionic Liquids: Physicochemical Properties, 1st ed., Elsevier Science, 2009.

[30] A.P. Korotkov, E.B. Bezlepkina, B.B. Damaskin, E.F. Golov, The effects of crystallographic surface inhomogeneity on double-layer structure and adsorption properties of cadmium electrodes, 1986.

[31] E. Lust, A. Jänes, K. Lust, M. Väärtnõu, Electric double layer structure and adsorption of cyclohexanol on single crystal cadmium, antimony and bismuth electrodes, Electrochim. Acta. 42 (1997) 771–783.

[32] R.R. Nazmutdinov, T.T. Zinkicheva, M. Probst, K. Lust, E. Lust, Adsorption of halide ions from aqueous solutions at a Cd(0 0 0 1) electrode surface: quantum chemical modelling and experimental study, Surface Science. 577 (2005) 112–126.

[33] L. Siinor, V. Ivaništšev, K. Lust, E. Lust, Impedance study of adsorption of iodide ions at Cd(0001) and Bi(111) electrode from various solutions with constant ionic strength, J. Solid State Electr. 14 (2010) 555–563.

[34] A. Nilsson, L. Pettersson, J.K. Nørskov, S. (Online service), Chemical bonding at surfaces and interfaces, Elsevier Amsterdam, 2008.

[35] E. Lust, In: Gileadi E, Urbakh M, Bard AJ, Stratmann M (eds) Encyclopedia of

electrochemistry, vol 1, Wiley-VCH, Weinheim, 2002.

[36] S. Trasatti, E. Lust, In: White RE, Conway BE, Bockris JO'M (eds) Modern aspects of electrochemistry, vol 33, Kluwer/Plenum, New York, 1999.

[37] Y. Lauw, M.D. Horne, T. Rodopoulos, A. Nelson, F.A.M. Leermakers, Electrical Double-Layer Capacitance in Room Temperature Ionic Liquids: Ion-Size and Specific Adsorption Effects, J. Phys. Chem. B. 114 (2010) 11149–11154.

[38] A.A. Kornyshev, Double-Layer in Ionic Liquids: Paradigm Change?, J. Phys. Chem. B. 111 (2007) 5545–5557.

[39] J.O.. Bockris, A.K.. Reddy, Modern electrochemistry, Springer Us, 2000.

[40] D. Henderson, S. Lamperski, Simple Description of the Capacitance of the Double Layer of a High Concentration Electrolyte, J. Chem. Eng. Data. 56 (2011) 1204–1208.

[41] M.S. Kilic, M.Z. Bazant, A. Ajdari, Steric effects in the dynamics of electrolytes at large applied voltages. I. Double-layer charging, Phys. Rev. E. 75 (2007) 021502.

[42] M.S. Kilic, M.Z. Bazant, A. Ajdari, Steric effects in the dynamics of electrolytes at large applied voltages: II. Modified Poisson-Nernst-Planck equations, Phys. Rev. E. 75 (2007) 021503.

[43] K.B. Oldham, A Gouy-Chapman-Stern model of the double layer at a metal/ionic liquid interface, J. Electroanal. Chem. 613 (2008) 131–138.

[44] D. Jiang, D. Meng, J. Wu, Density functional theory for differential capacitance of planar electric double layers in ionic liquids, Chem. Phys. Lett. 504 (2011) 153–158.

[45] J. Forsman, C.E. Woodward, M. Trulsson, A Classical Density Functional Theory of Ionic Liquids, J. Phys. Chem. B. 115 (2011) 4606–4612.

[46] J. Wu, T. Jiang, D. Jiang, Z. Jin, D. Henderson, A classical density functional theory for interfacial layering of ionic liquids, Soft Matter. 7 (n.d.) 11222–11231.

[47] D. Henderson, S. Lamperski, Z. Jin, J. Wu, Density Functional Study of the Electric Double Layer Formed by a High Density Electrolyte, J. Phys. Chem. B. 115 (2011) 12911–12914.

[48] S.K. Reed, O.J. Lanning, P.A. Madden, Electrochemical interface between an ionic liquid and a model metallic electrode, J. Chem. Phys. 126 (2007) 084704–13.

[49] M.V. Fedorov, A.A. Kornyshev, Towards understanding the structure and capacitance of electrical double layer in ionic liquids, Electrochim. Acta. 53 (2008) 6835–6840.

[50] S.A. Kislenko, R.H. Amirov, I.S. Samoylov, Influence of temperature on the structure and dynamics of the [BMIM][PF6] ionic liquid/graphite interface, Phys. Chem. Chem. Phys. 12 (2010) 11245–11250.

[51] S. Tazi, M. Salanne, C. Simon, P. Turq, M. Pounds, P.A. Madden, Potential-Induced Ordering Transition of the Adsorbed Layer at the Ionic Liquid/Electrified Metal Interface, J. Phys. Chem. B. 114 (2010) 8453–8459.

[52] M.V. Fedorov, N. Georgi, A.A. Kornyshev, Double layer in ionic liquids: The nature of the camel shape of capacitance, Electr. Commun. 12 (2010) 296–299.

[53] M. Trulsson, J. Algotsson, J. Forsman, C.E. Woodward, Differential Capacitance of Room Temperature Ionic Liquids: The Role of Dispersion Forces, J. Phys. Chem. Lett. 1 (2010) 1191–1195.

[54] J. Vatamanu, O. Borodin, G.D. Smith, Molecular Insights into the Potential and Temperature Dependences of the Differential Capacitance of a Room-Temperature Ionic Liquid at Graphite Electrodes, J. Am. Chem. Soc. 132 (2010) 14825–14833.

[55] Q. Dou, M.L. Sha, H.Y. Fu, G.Z. Wu, Molecular dynamics simulation of the interfacial structure of [CnMIm][PF6] adsorbed on a graphite surface: effects of temperature and alkyl chain length, Journal of Physics: Condensed Matter. 23 (2011) 175001.

[56] E. Soolo, D. Brandell, A. Liivat, H. Kasemägi, T. Tamm, A. Aabloo, Molecular dynamics simulations of EMI-BF4 in nanoporous carbon actuators, J. Mol. Model. (2011).

[57] B. Roling, M. Drüschler, B. Huber, Slow and fast capacitive process taking place at the ionic liquid/electrode interface, Faraday Discuss. (2012).

[58] T. Pajkossy, D.M. Kolb, The interfacial capacitance of Au(100) in an ionic liquid, 1-butyl-3-methyl-imidazolium hexafluorophosphate, Electr. Commun. 13 (2011) 284–286.

[59] M.M. Islam, M.T. Alam, T. Ohsaka, Electrical Double-Layer Structure in Ionic Liquids: A Corroboration of the Theoretical Model by Experimental Results, J. Phys. Chem. C. 112 (2008) 16568–16574.

[60] M.M. Islam, M.T. Alam, T. Okajima, T. Ohsaka, Electrical Double Layer Structure in Ionic Liquids: An Understanding of the Unusual Capacitance−Potential Curve at a Nonmetallic Electrode, J. Phys. Chem. C. 113 (2009) 3386–3389.

[61] V. Lockett, M. Horne, R. Sedev, T. Rodopoulos, J. Ralston, Differential capacitance of the double layer at the electrode/ionic liquids interface, Phys. Chem. Chem. Phys. 12 (2010) 12499.

[62] T.R. Gore, T. Bond, W. Zhang, R.W.J. Scott, I.J. Burgess, Hysteresis in the measurement of double-layer capacitance at the gold-ionic liquid interface, Electrochem. Commun. 12 (2010) 1340–1343.

[63] M.H. Ghatee, F. Moosavi, Physisorption of Hydrophobic and Hydrophilic 1-Alkyl-3-methylimidazolium Ionic Liquids on the Graphenes, J. Phys. Chem. C. 115 (2011) 5626–5636.

[64] T.P.C. Klaver, M. Luppi, M.H.F. Sluiter, M.C. Kroon, B.J. Thijsse, DFT Study of 1,3-Dimethylimidazolium Tetrafluoroborate on Al and Cu(111) Surfaces, J. Phys. Chem. C. 115 (2011) 14718–14730.

[65] H. Valencia, M. Kohyama, S. Tanaka, H. Matsumoto, Ab initio study of EMIM-BF4 crystal interaction with a Li(100) surface as a model for ionic liquid/Li interfaces in Li-ion batteries, J. Chem. Phys. 131 (2009) 244705.

[66] H. Valencia, M. Kohyama, S. Tanaka, H. Matsumoto, Ab initio study of EMIM-BF4 molecule adsorption on Li surfaces as a model for ionic liquid/Li interfaces in Li-ion batteries, Phys. Rev. B. 78 (2008) 205402.

[67] S. Baldelli, Surface Structure at the Ionic Liquid−Electrified Metal Interface, Acc. Chem. Res. 41 (2008) 421–431.

[68] X. Si, S. Li, Y. Wang, S. Ye, T. Yan et al., Effects of Specific Adsorption on the Differential Capacitance of Imidazolium-Based Ionic Liquid Electrolytes, Chem. Phys. Chem. (2012).

[69] F. Endres, S.Z.E. Abedin, Air and water stable ionic liquids in physical chemistry, Phys. Chem. Chem. Phys. 8 (2006) 2101–2116.

[70] E. Barsoukov, J.R. Macdonald, Impedance spectroscopy: theory, experiment, and applications, Wiley, John & Sons, Incorporated, 2005.

[71] S.S. Moganty, R.E. Baltus, D. Roy, Electrochemical windows and impedance characteristics of [Bmim+][BF4-] and [Bdmim+][BF4-] ionic liquids at the surfaces of Au, Pt, Ta and glassy carbon electrodes, Chem. Phys. Lett. 483 (2009) 90–94.

[72] M. Drüschler, B. Huber, B. Roling, On Capacitive Processes at the Interface between 1-Ethyl-3-methylimidazolium tris(pentafluoroethyl)trifluorophosphate and Au(111), J. Phys. Chem. C. 115 (2011) 6802–6808.

[73] A. Stoppa, O. Zech, W. Kunz, R. Buchner, The Conductivity of Imidazolium-Based Ionic Liquids from (−35 to 195) °C. A. Variation of Cation's Alkyl Chain, J. Chem. Eng. Data. 55 (2009) 1768–1773.

[74] O. Zech, A. Stoppa, R. Buchner, W. Kunz, The Conductivity of Imidazolium-Based Ionic Liquids from (248 to 468) K. B. Variation of the Anion, J. Chem. Eng. Data. 55 (2010) 1774–1778.

[75] G.-B. Pan, W. Freyland, 2D phase transition of PF6 adlayers at the electrified ionic liquid/Au(111) interface, Chem. Phys. Lett. 427 (2006) 96–100.

[76] Y. Su, Y. Fu, J. Yan, Z. Chen, B. Mao, Double Layer of Au(100)/Ionic Liquid Interface and Its Stability in Imidazolium-Based Ionic Liquids, Angew. Chem. 121 (2009) 5250–5253.

[77] N. Borisenko, S. Zein El Abedin, F. Endres, An in Situ STM and DTS Study of the Extremely Pure [EMIM]FAP/Au(111) Interface, Chem. Phys. Chem. (2011).

[78] F. Endres, N. Borisenko, S.Z.E. Abedin, R. Hayes, R. Atkin, The interface ionic liquid(s)/electrode(s): In situ STM and AFM measurements, Faraday Discuss. (2012).

[79] R. Atkin, S.Z.E. Abedin, R. Hayes, L.H.S. Gasparotto, N. Borisenko, F. Endres, AFM and STM Studies on the Surface Interaction of [BMP]TFSA and [EMIm]TFSA Ionic Liquids with Au(111), J. Phys. Chem. C. 113 (2009) 13266–13272.

[80] T. Carstens, R. Hayes, S.Z.E. Abedin, B. Corr, G.B. Webber, N. Borisenko, et al., In situ STM, AFM and DTS study of the interface 1-hexyl-3-methylimidazolium tris(pentafluoroethyl)trifluorophosphate/Au(111), Electrochim. Acta. (n.d.).

[81] R.M. Lynden-Bell, A.I. Frolov, M. Fedorov, Electrode Screening by Ionic Liquids, Phys. Chem. Chem. Phys. (2011).

[82] M.Z. Bazant, B.D. Storey, A.A. Kornyshev, Double Layer in Ionic Liquids: Overscreening versus Crowding, Phys. Rev. Lett. 106 (2011) 046102.

[83] R. Finken, V. Ballenegger, J.-P. Hansen, Onsager model for a variable dielectric permittivity near an interface, Mol. Phys. 101 (2003) 2559–2568.

[84] M. Holovko, V. Kapko, D. Henderson, D. Boda, On the influence of ionic association on the capacitance of an electrical double layer, Chem. Phys. Lett. 341 (2001) 363–368.

[85] K. Dong, S. Zhang, Hydrogen Bonds: A Structural Insight into Ionic Liquids, Chemistry - A European Journal. 18 (2012) 2748–2761.

[86] W. Zhao, F. Leroy, B. Heggen, S. Zahn, B. Kirchner, S. Balasubramanian, et al., Are There Stable Ion-Pairs in Room-Temperature Ionic Liquids? Molecular Dynamics Simulations of 1-n-Butyl-3-methylimidazolium Hexafluorophosphate, J. Am. Chem. Soc. 131 (2009) 15825–15833.

[87] G. Feng, J. Huang, B.G. Sumpter, V. Meunier, R. Qiao, A “counter-charge layer in generalized solvents” framework for electrical double layers in neat and hybrid ionic liquid electrolytes, Phys. Chem. Chem. Phys. (2011).

KOKKUVÕTE

Ioonide adsorptsioon Cd(0001) elektroodil ioonsetest vedelikest erinevatel temperatuuridel.

Anton Ruzanov

Tsüklilise voltamperomeetria ja elektrokeemilise impedantsspektroskoopia (EIS) meetoditega uuriti protsesse ioonse vedeliku (1-etüül-3-methüülimidasoolium tetrafluoroboraat, $EMImBF_4$) ja Cd(0001) elektroodi piirpinnal erinevatel elektroodi potentsiaalidel ja temperatuuridel. Uuringud on vajalikud elektroodi ja ioonse vedeliku (RTIL) piirpinna struktuuri kirjeldamiseks, mis omakorda on oluline erinevatel piirpindadel toimuvate protsesside modelleerimiseks.

Cd(0001) | $EMImBF_4$ piirpinna mahtuvusliku takistuse aktiivtakistusest sõltuvuste (nn. Nyquisti sõltuvuste) analüüs näitas head reprodutseeritavust kõrgematel vahelduvvoolu sagedustel. Madalamatel sagedustel on näha tulemuste suuremat hajuvust. Faasinurga sagedusest sõltuvused näitasid, et kõrgetel sagedustel toimub kiire elektrilise kaksikkihi moodustumine, kuid keskmistel sagedustel limiteerib elektroodi käitumist adsorptsioon ning madalatel sagedustel saavad järjest olulisemaks massiülekande- (diffusioon) ja laenguülekandeprotsessid. Madalamate sageduste alas kogu potentsiaalivahemikus näitavad faasinurga sagedusest sõltuvused, et mida kõrgem on temperatuur, seda suurem mõju on ka laenguülekandeprotsessidel. Sagedustel 10–100 Hz on faasiunurga absoluutväärtus seda suurem, mida madalam on temperatuur, st seda väiksemad on kõrvalekalded ideaalsest adsorptsioonilisest käitumisest.

EIS spektreid modelleeriti modifitseeritud Grafov-Damaskini mudeliga ning määrati Cd(0001) | $EMImBF_4$ piirpinda iseloomustavad parameetrid. Leiti, et nii elektrilise kaksikkihi tõeline mahtuvus (C_{dl}) kui ka adsorptsiooniline mahtuvus (C_{ad}) suurenevad temperatuuri tõstmisel, mis viitab sellele, et elektroodilähedase elektrolüüdikihi struktuur sõltub samuti temperatuurist. Cd(0001) elektroodi null-laengu potentsiaal $EMImBF_4$-s asub E = –0.8 V lähedal, kus C_{ad}, C_{dl} ja R_D on maksimaalsed. C_{ad} ja C_{dl} väärtused on vastavalt madalatel sagedustel takistatud osalise laenguülekande takistusega (R_{ct}) ning kõrgetel sagedustel elektrolüüdi takistusega (R_{el}). Nii R_{el} kui R_{ct} sõltuvad tugevasti temperatuurist, mis viitab sellele, et need on kineetilised parameetrid. R_{ct} sõltuvus temperatuurist iseloomustab RTIL kihtide struktuuri elektroodi pinna lähedal. R_{el} ja R_{ct}-ga iseloomustatavate protsesside

aktivatsioonienergiad on E_{el} = 8 kJ/mol and E_{ct} = 12 kJ/mol. R_{ct}-ga kirjeldatava protsessi aktivatsioonienergia veidi suurem väärtus viitab sellele, et laetud osakeste liikumine elektroodilähedases kihis on raskendatud, sest see osa ioonsest vedelikust on rohkem struktureeritud.

RTIL struktuur kujutab hästi korrastatud ala elektroodi pinna lähedal. Faasidevahelise piirpinna struktuur sõltub RTIL keemilisest koostisest (katiooni ja aniooni struktuurist), potentsiaalist, temperatuurist ja lisandite olemasolust. Paljud uuringud on näidanud, et faasidevahelise piirpinna moodustumine on väga aeglane ja ioonid liikumine on raskendatud. Madalatel temperatuuridel ning kõrgete potentsiaalide korral on RTIL elektroodi pinna lähedal klaasi sarnase struktuuriga, mis muutub seda kiiremini, mida kõrgem on temperatuur ja väiksem on potentsiaali erinevus null-laengu potentsiaalist. See, kuidas metall | RTIL piirpinna lähedane struktuur sõltub temperatuurist, püüavad kirjeldada mitmed kaasaegsed teooriad. Üks neist on kombineeritud MSA-MAL teooria (MSA – mean spherical approximation; MAL – mass-action law), mille alusel ei ole kõik ioonid ioonses vedelikus „vabad“, vaid teatud osa esineb ioonpaaridena. Mida kõrgem on temperatuur, seda rohkem on „vabu“ ioone ning süsteemi mahtuvuslikud omadused lähenevad elektrolüütide klassikalisele käitumisele. MSA-MAL teooria ennustab kvalitatiivselt metall | RTIL piirpinna omadusi, mida kinnitavad ka antud töös saadud eksperimentaalsed andmed. Kuna tegemist on väga komplitseeritud ja seni vähe uuritud teemaga, siis tuleb kindlasti teha lisauuringuid.

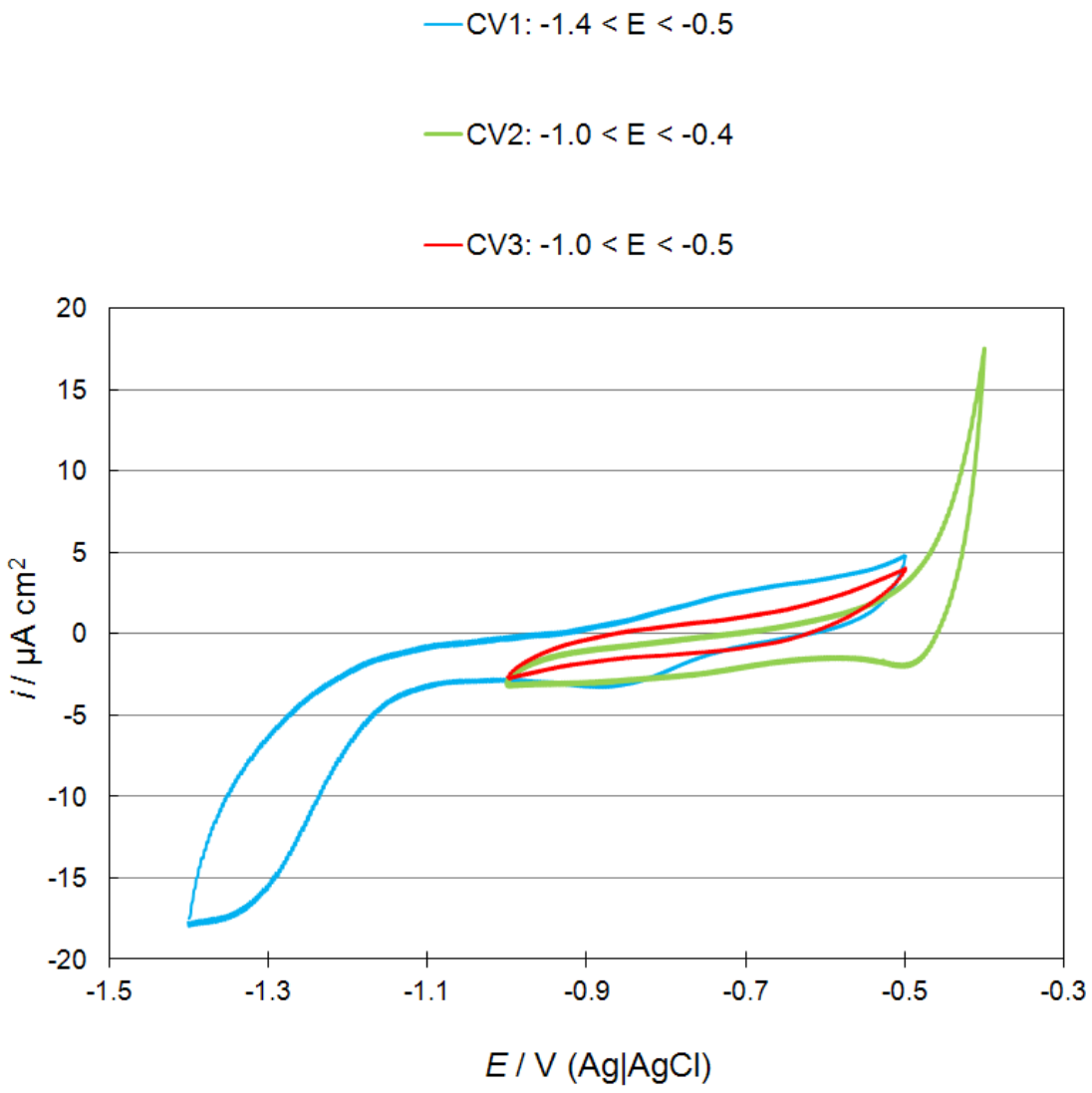

Figure 1: Cyclic voltammograms for Cd(0001) in $EMImBF_4$ at scan rate of $\nu = 20$ mVs^{-1}.

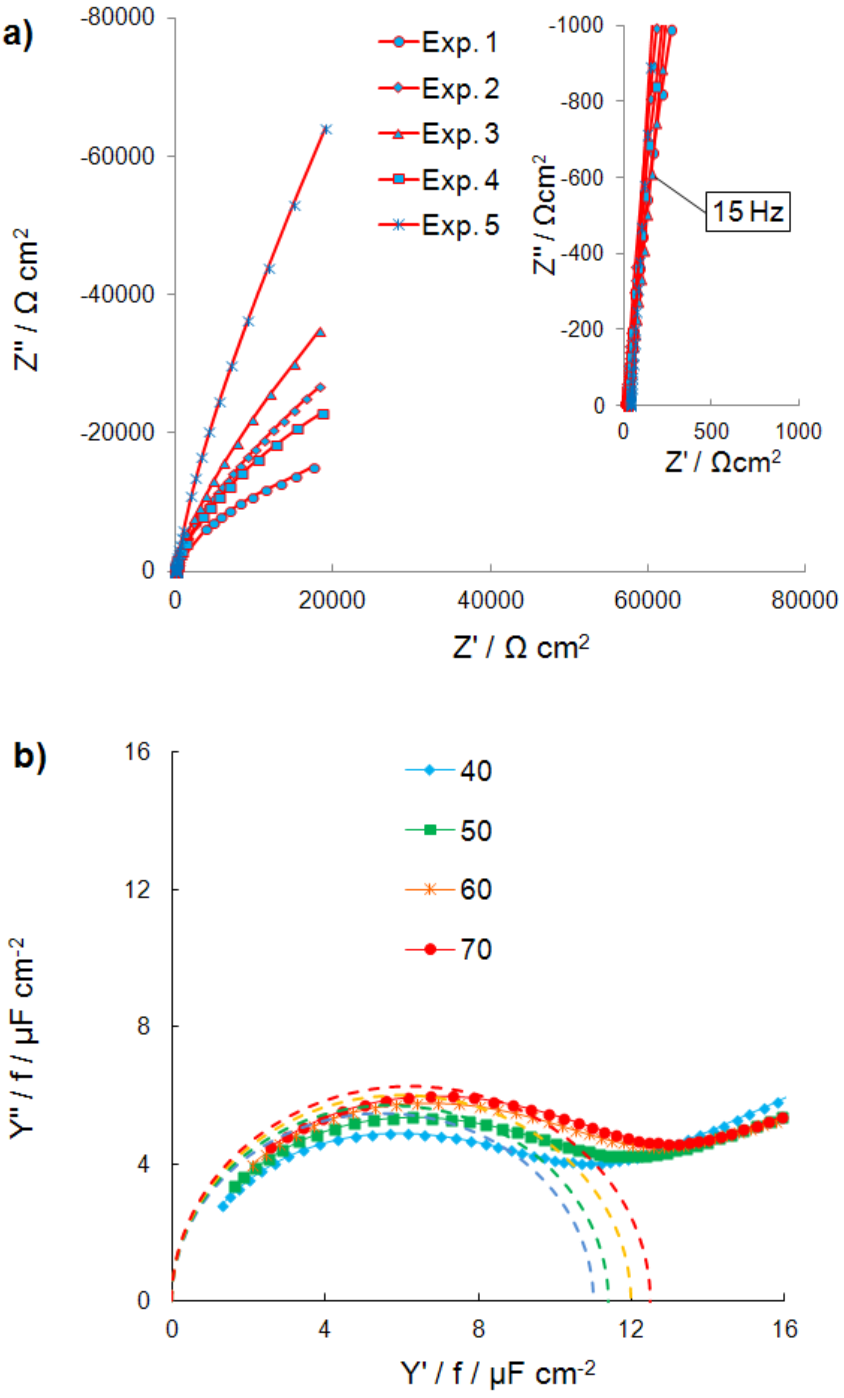

Figure 2: a) *Z''*, *Z'*– dependencies (*t* = 30 °C, *E* = –0.8 V) for different experiments (indicated in figure). **b)** *Y''/f*, *Y'/f* - dependencies (*E* = –0.8 V) at different temperatures (indicated in figure).

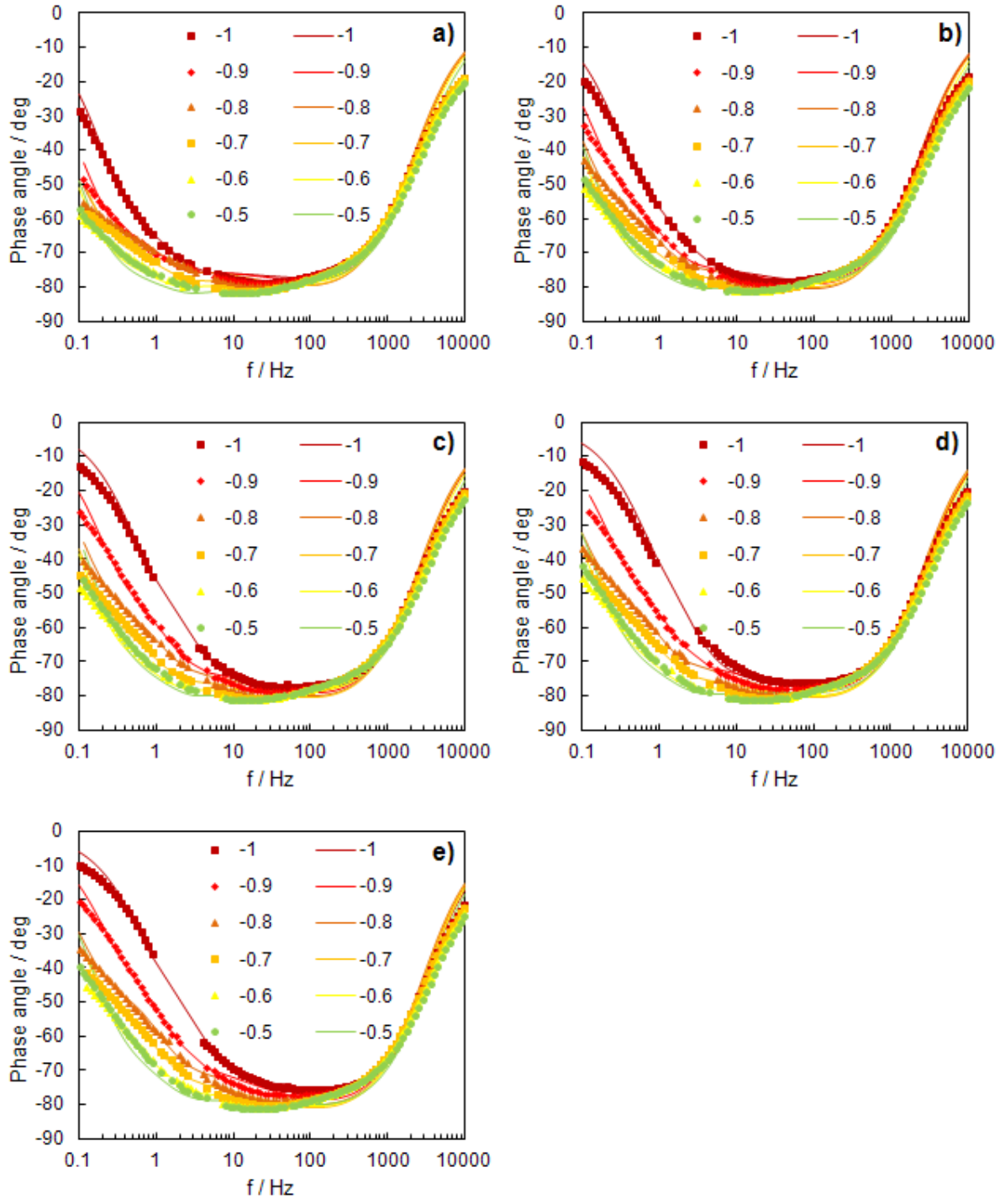

Figure 3: The phase angle dependence on frequency at different potentials (indicated in figure) and various fixed temperatures (°C): **a)** 30; **b)** 40; **c)** 50; **d)** 60; **e)** 70.

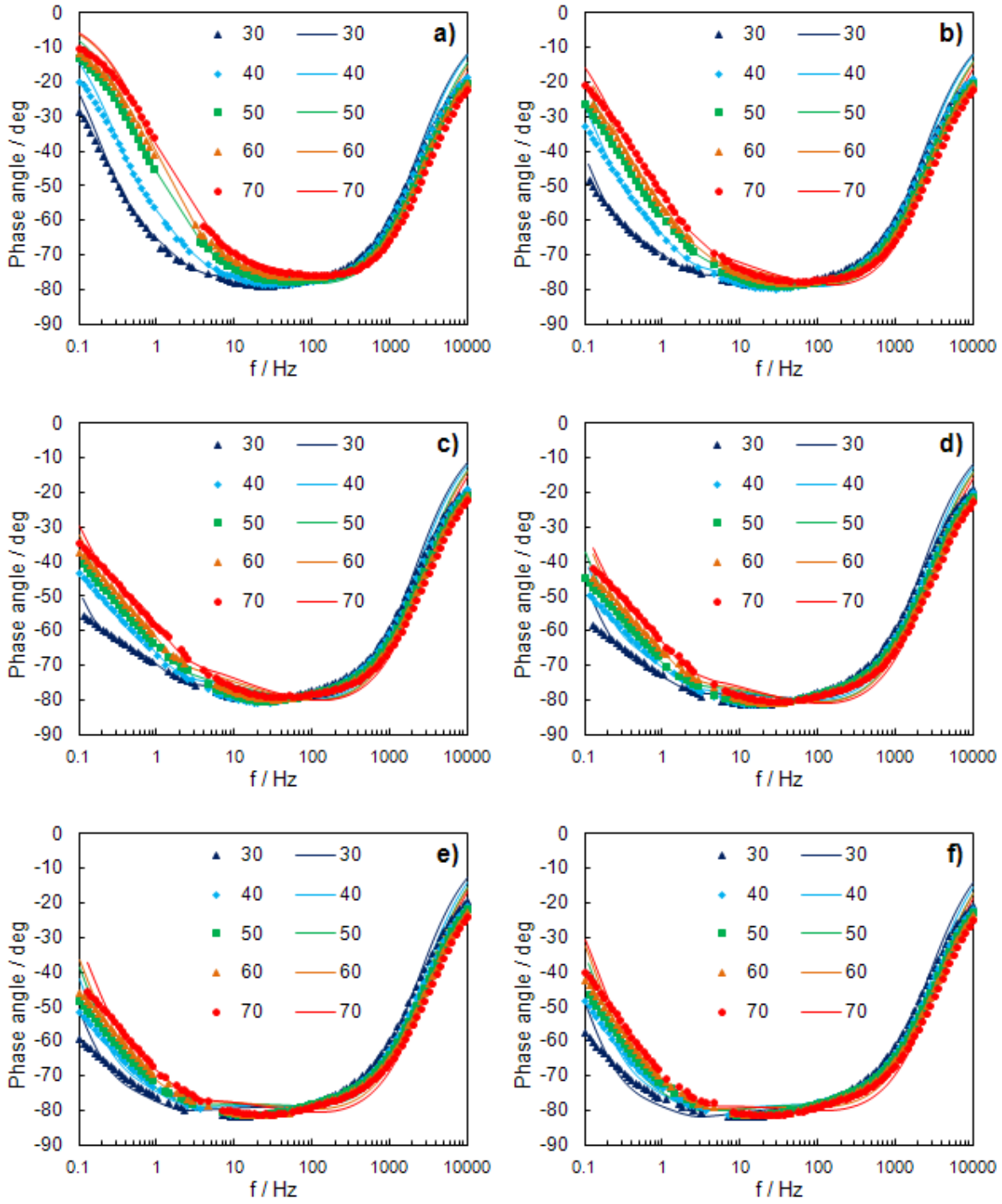

Figure 4: The phase angle dependence on frequency at various fixed potentials (V vs. Ag | AgCl): **a)** –1.0; **b)** –0.9; **c)** –0.8; **d)** –0.7; **e)** –0.6; **f)** –0.5 and different temperatures (indicated in figure).

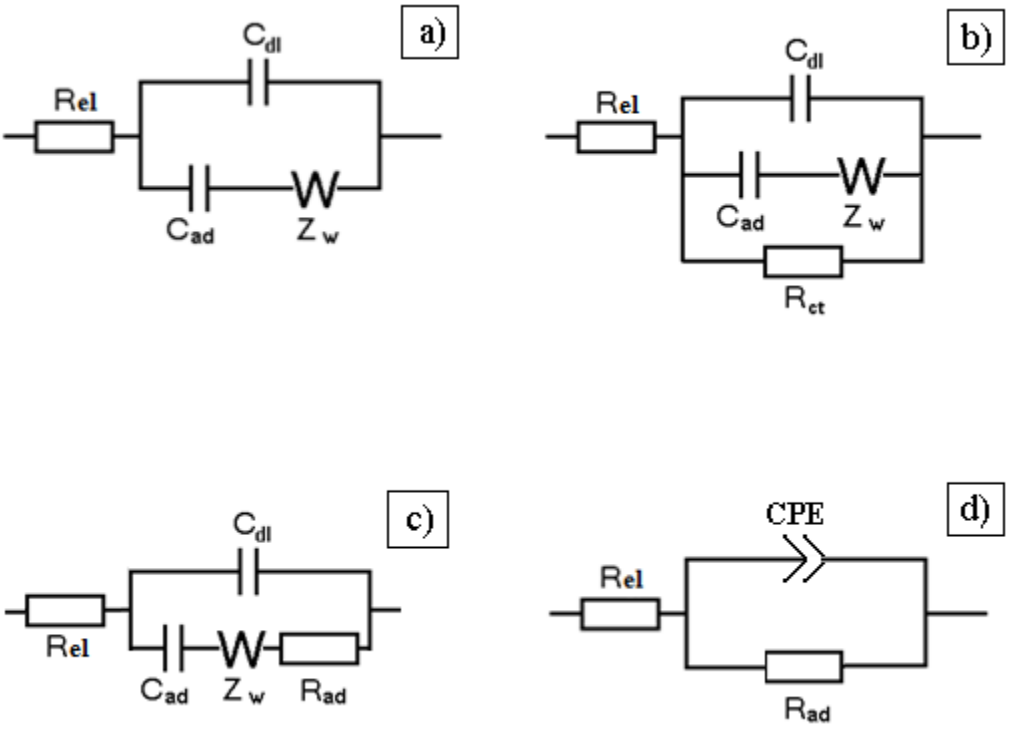

Figure 5: The experimental impedance data were mainly analysed using this equivalent circuits, where: R_{el} – electrolyte resistance, C_{dl} – electrical double-layer capacitance, C_{ad} – adsorption capacitance, R_{ad} – adsorption resistance, R_{ct} – partial charge transfer resistance, Z_w – Warburg diffusion impedance, CPE – constant phase element.

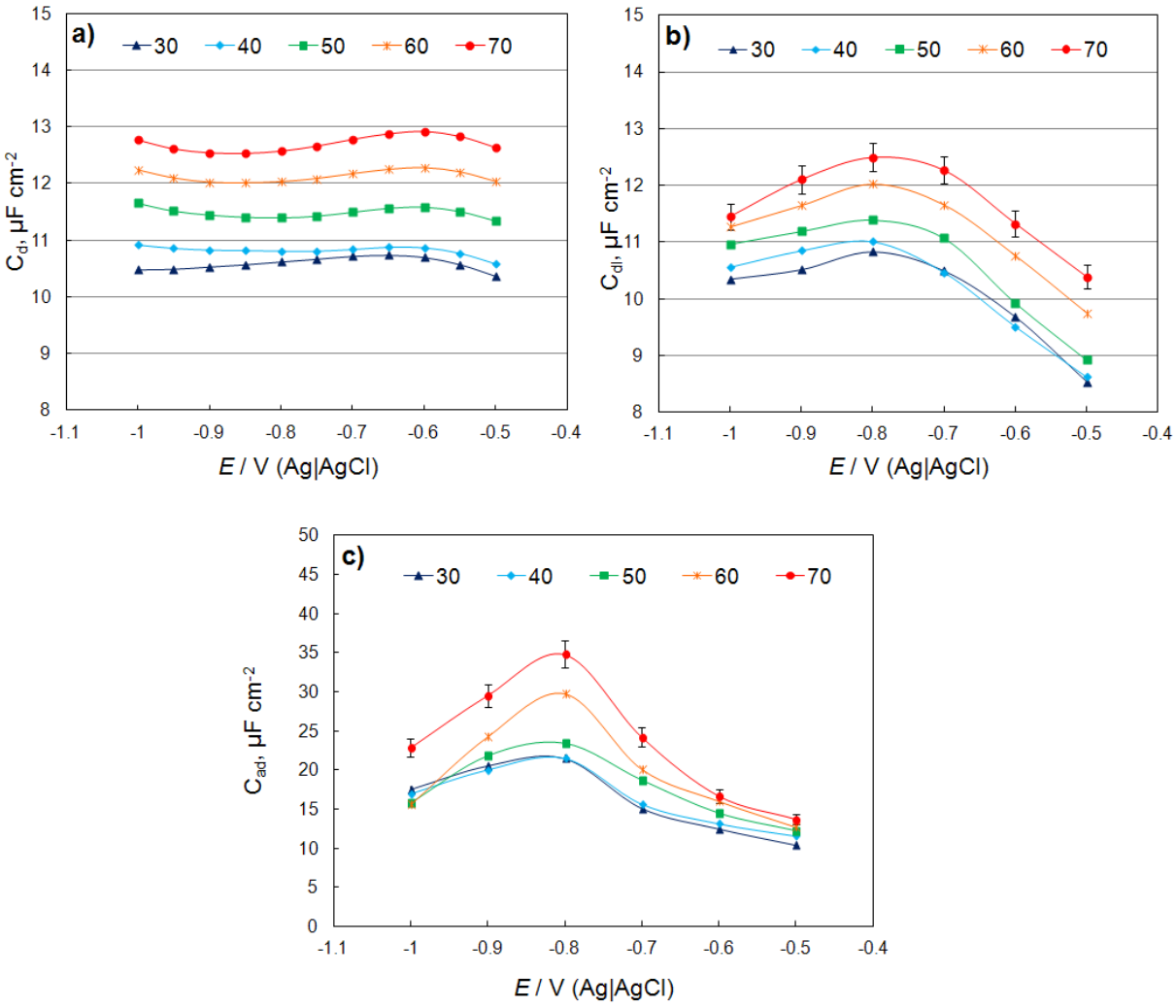

Figure 6: The dependences of **a)** differential capacitance (C_d) (f = 201 Hz) **b)** high-frequency or EDL real capacitance (C_{dl}) and **c)** adsorption capacitance (C_{ad}) on the Cd(0001) electrode potential in $EMImBF_4$ at different temperatures (indicated in Figure). C_{dl} and C_{ad} have been found by impedance spectra modelling.

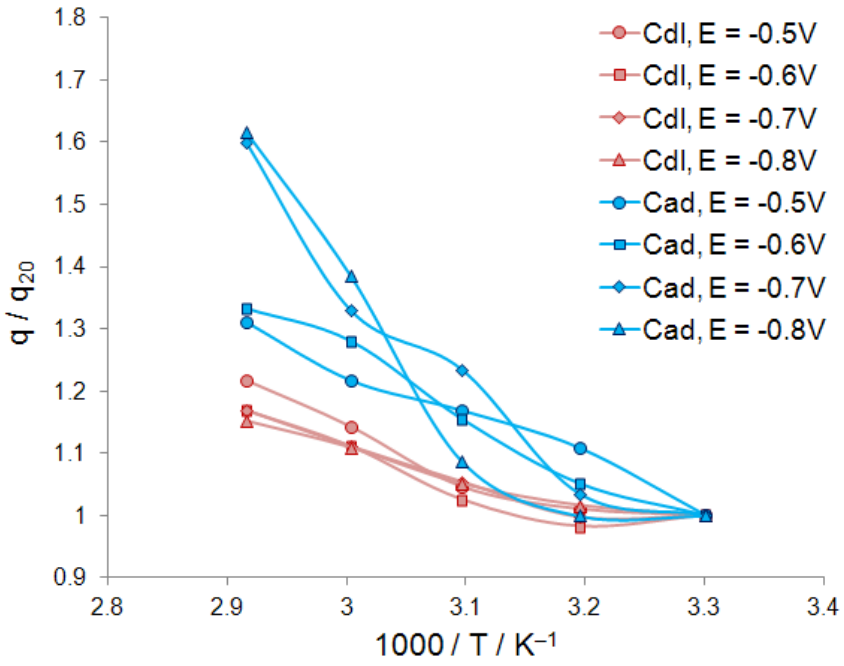

Figure 7: The fitted quantities − q (C_{dl} and C_{ad} capacitances) divided by their value at 20 °C − q_{20}, as a function of temperature (in Arrhenius representation).

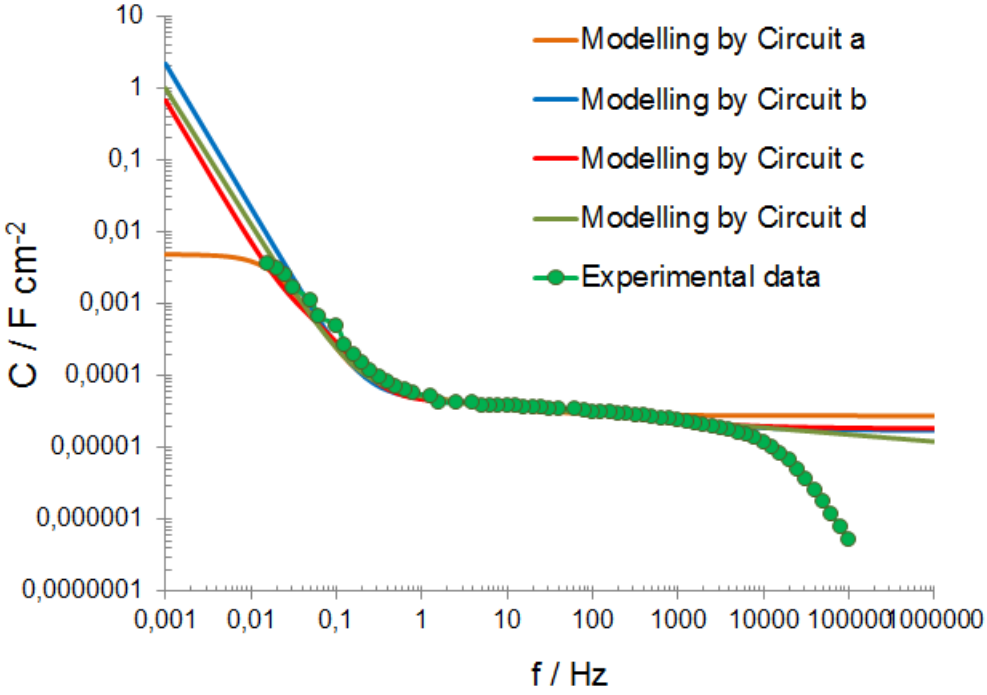

Figure 8: The dependence of the sum of C_{dl} and C_{ad} capacitances on frequency.

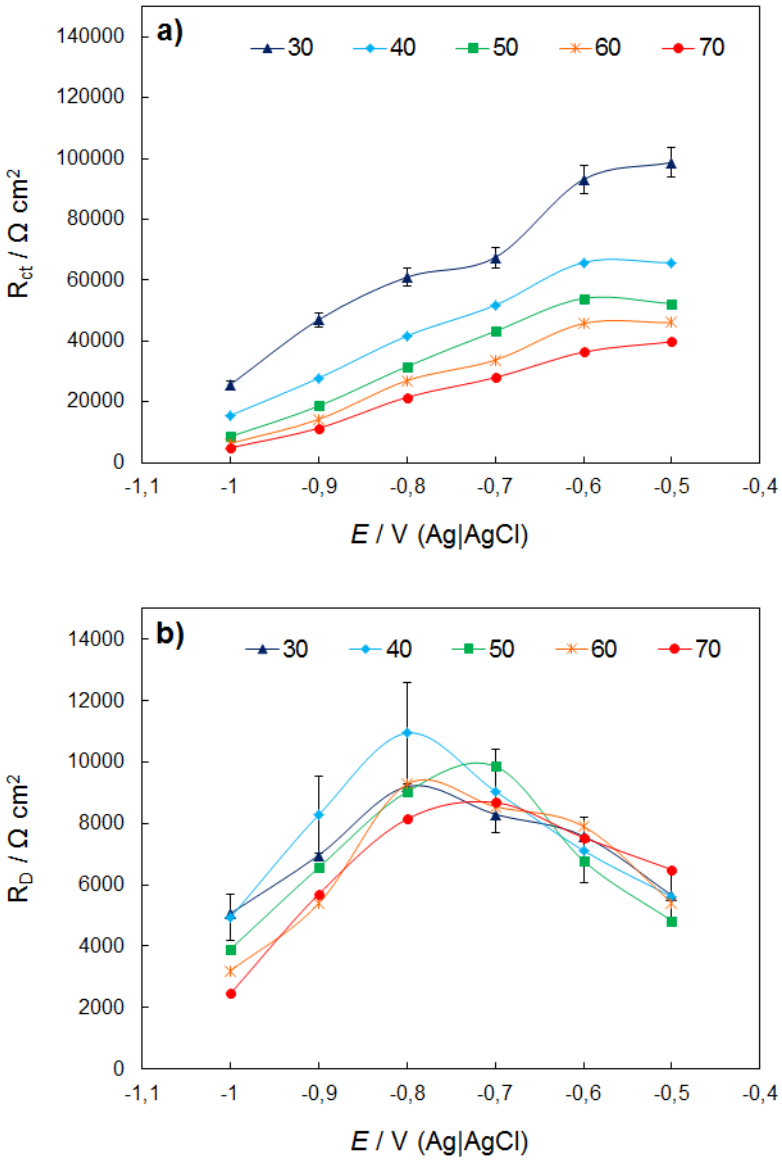

Figure 9: a) The charge transfer resistance (R_{ct}) and **b)** the diffusion resistance (R_D) vs. electrode potential dependences for Cd(0001) in $EMImBF_4$ at different temperatures (indicated in figure).

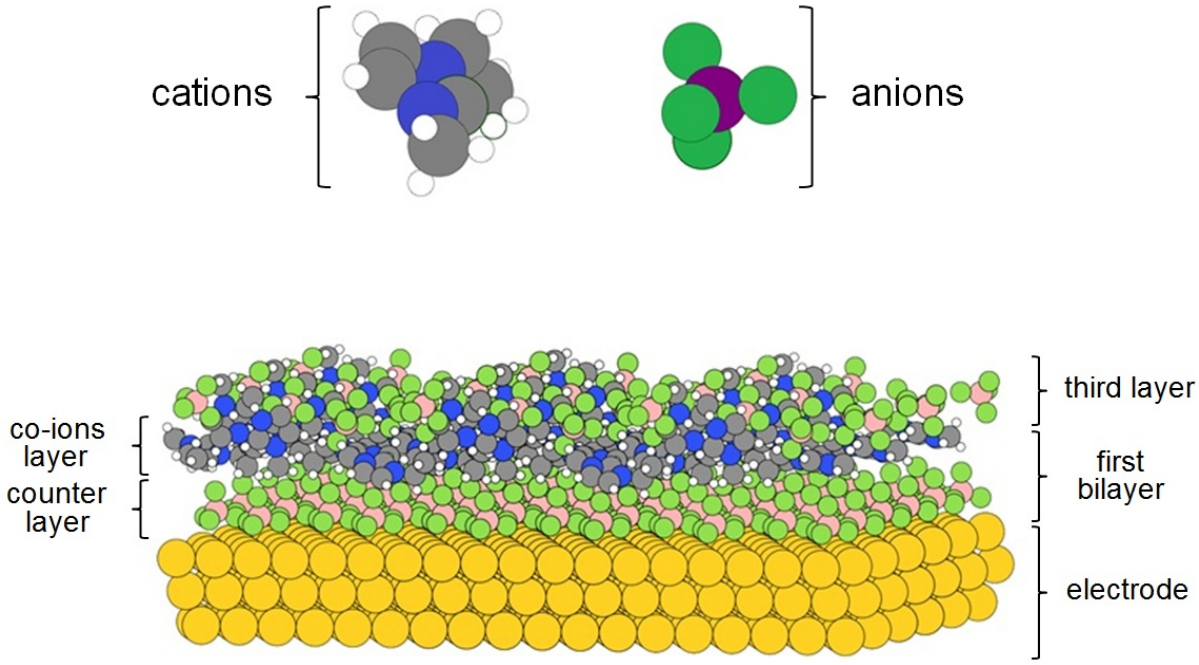

Figure 10: RTIL structure near electrode surface.

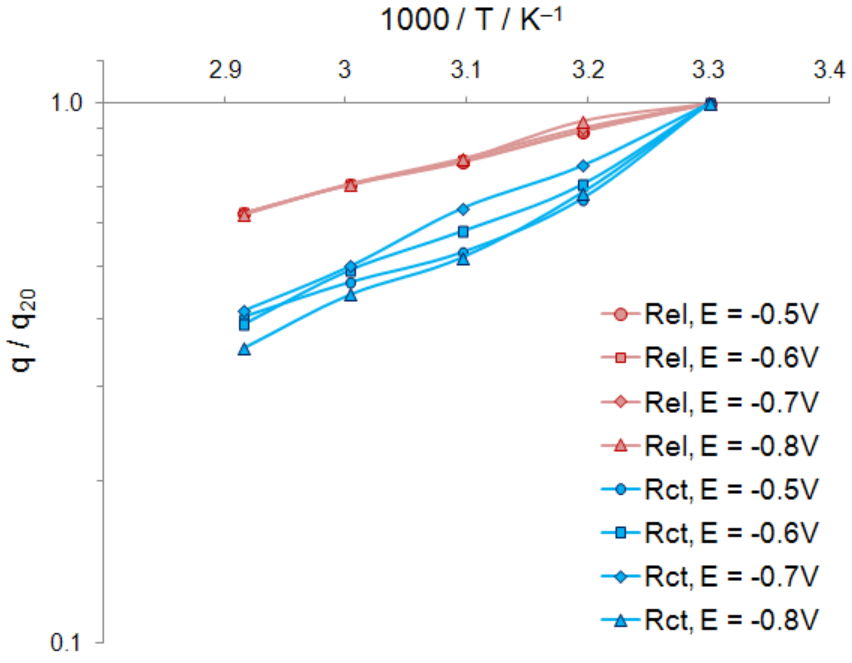

Figure 11: The fitted quantities − q (R_{el} and R_{ct} resistances) divided by their value at 20 °C − q_{20}, as a logarithmic function of temperature (in Arrhenius representation).